08-09 August 2009

TECH BRIEFS

NATIONAL AERONAUTICS AND SPACE ADMINISTRATION

INTRODUCTION

Tech Briefs are short announcements of innovations originating from research and development activities of the National Aeronautics and Space Administration. They emphasize information considered likely to be transferable across industrial, regional, or disciplinary lines and are issued to encourage commercial application.

Availability of NASA Tech Briefs and TSPs

Requests for individual Tech Briefs or for Technical Support Packages (TSPs) announced herein should be addressed to

National Technology Transfer Center

Telephone No. **(800) 678-6882** or via World Wide Web at **www2.nttc.edu/leads/**

Please reference the control numbers appearing at the end of each Tech Brief. Information on NASA's Innovative Partnerships Program (IPP), its documents, and services is also available at the same facility or on the World Wide Web at **http://ipp.nasa.gov**.

Innovative Partnerships Offices are located at NASA field centers to provide technology-transfer access to industrial users. Inquiries can be made by contacting NASA field centers listed below.

NASA Field Centers and Program Offices

Ames Research Center
Lisa L. Lockyer
(650) 604-1754
lisa.l.lockyer@nasa.gov

Dryden Flight Research Center
Gregory Poteat
(661) 276-3872
greg.poteat@dfrc.nasa.gov

Glenn Research Center
Kathy Needham
(216) 433-2802
kathleen.k.needham@nasa.gov

Goddard Space Flight Center
Nona Cheeks
(301) 286-5810
nona.k.cheeks@nasa.gov

Jet Propulsion Laboratory
Andrew Gray
(818) 354-3821
gray@jpl.nasa.gov

Johnson Space Center
information
(281) 483-3809
jsc.techtran@mail.nasa.gov

Kennedy Space Center
David R. Makufka
(321) 867-6227
david.r.makufka@nasa.gov

Langley Research Center
Brian Beaton
(757) 864-2192
brian.f.beaton@nasa.gov

Marshall Space Flight Center
Jim Dowdy
(256) 544-7604
jim.dowdy@msfc.nasa.gov

Stennis Space Center
Ramona Travis
(228) 688-3832
ramona.e.travis@nasa.gov

Carl Ray, Program Executive
Small Business Innovation Research (SBIR) & Small Business Technology Transfer (STTR) Programs
(202) 358-4652
carl.g.ray@nasa.gov

Doug Comstock, Director
Innovative Partnerships Program Office
(202) 358-2560
doug.comstock@nasa.gov

TECH BRIEFS

NATIONAL AERONAUTICS AND SPACE ADMINISTRATION

Aligning a Receiving Antenna Array To Reduce Interference

This arraying algorithm has potential utility in radio astronomy and radio communication.

NASA's Jet Propulsion Laboratory, Pasadena, California

A digital signal-processing algorithm has been devised as a means of aligning (as defined below) the outputs of multiple receiving radio antennas in a large array for the purpose of receiving a desired weak signal transmitted by a single distant source in the presence of an interfering signal that (1) originates at another source lying within the antenna beam and (2) occupies a frequency band significantly wider than that of the desired signal. In the original intended application of the algorithm, the desired weak signal is a spacecraft telemetry signal, the antennas are spacecraft-tracking antennas in NASA's Deep Space Network, and the source of the wide-band interfering signal is typically a radio galaxy or a planet that lies along or near the line of sight to the spacecraft. The algorithm could also afford the ability to discriminate between desired narrow-band and nearby undesired wide-band sources in related applications that include satellite and terrestrial radio communications and radio astronomy.

The development of the present algorithm involved modification of a prior algorithm called "SUMPLE" and a predecessor called "SIMPLE." SUMPLE was described in "Algorithm for Aligning an Array of Receiving Radio Antennas" (NPO-40574), *NASA Tech Briefs* Vol. 30, No. 4 (April 2006), page 54. To recapitulate: As used here, "aligning" signifies adjusting the delays and phases of the outputs from the various antennas so that their relatively weak replicas of the desired signal can be added coherently to increase the signal-to-noise ratio (SNR) for improved reception, as though one had a single larger antenna. Prior to the development of SUMPLE, it was common practice to effect alignment by means of a process that involves correlation of signals in pairs. SIMPLE is an example of an algorithm that effects such a process. SUMPLE also involves correlations, but the correlations are not performed in pairs. Instead, in a partly iterative process, each signal is appropriately weighted and then correlated with a composite signal equal to the sum of the other signals.

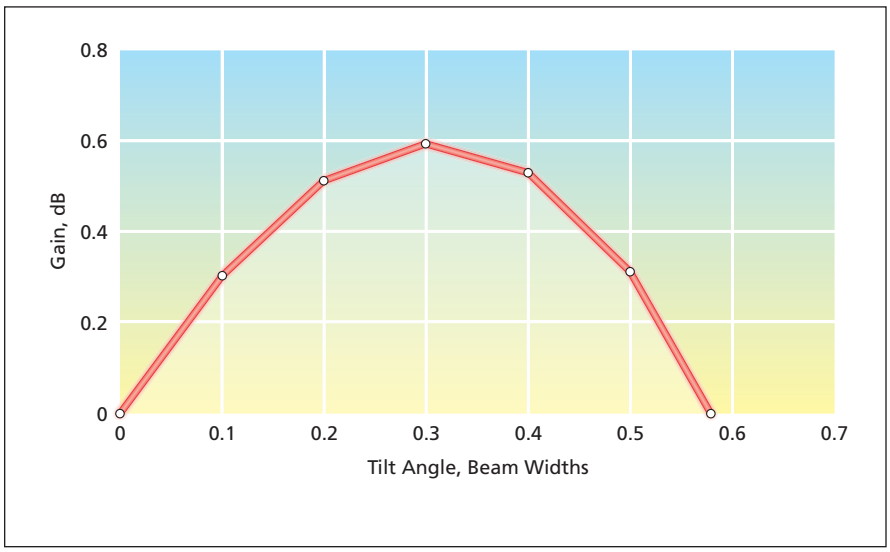

Tilting the Beam of an antenna array in a refinement of the present signal-processing algorithm can afford a small gain in SNR of the desired signal. Plotted here are results of a simulation in which the desired and interfering signals were both 5 dB above noise and were coming from the same direction.

For the purpose of the present algorithm, it is assumed that the receiver at each antenna is of a multi-channel type, so that its outputs can be processed to obtain a cross-correlation spectrum of the incoming signals. It is further assumed that the channels are configured to afford both sufficient resolution and sufficient bandwidth to accommodate the telemetry or other desired narrow-band signal by use of several of its inner channels while simultaneously accommodating the wide-band interfering signal, devoid of significant contribution from the desired narrow-band signal, by use of its remaining (outer) channels. Under this assumption, pertinent correlation characteristics of the interfering signal can be calculated by use of data from the outer channels only, then subtracted from the corresponding characteristics of the total signal in the inner channels, yielding desired-signal correlations without the interferer. The calculations include least-squares fits of phase-versus-frequency models for both the desired and the interfering signals, using all the channels. The fitting process enables estimation of residual delays for the desired and interfering signals when there is sufficient signal-to-noise ratio.

The algorithm as summarized thus far guarantees only that the array is aligned to form a pencil beam that points toward the source of the desired signal. The algorithm does not eliminate or reduce the effects of the interfering signal on the overall system noise. The algorithm does, however, provide an option for further refinement through adjustment of correlation weights so as to tilt and/or reshape the beam (see figure). Depending on the angular distribution of the interferer relative to the desired source and on relative strengths of the desired signal, the interfering signal, and noise, it may be possible to increase the SNR of the desired signal through such reshaping or tilting.

This work was done by Andre P. Jongeling of Caltech and David H. Rogstad of Santa Barbara Applied Research for NASA's Jet Propulsion Laboratory. For more information, contact iaoffice@jpl.nasa.gov. NPO-45640

Collecting Ground Samples for Balloon-Borne Instruments

Harpoonlike sample-collection devices would be dropped, then hauled back up.

NASA's Jet Propulsion Laboratory, Pasadena, California

A proposed system in a gondola containing scientific instruments suspended by a balloon over the surface of the Saturn moon Titan would quickly acquire samples of rock or ice from the ground below. Prototypes of a sample-collecting device that would be a major part of the system have been tested under cryogenic and non-cryogenic conditions on Earth. Systems like this one could also be used in non-cryogenic environments on Earth to collect samples of rock, soil, ice, mud, or other ground material from such inaccessible or hazardous locations as sites of suspected chemical spills or biological contamination.

The sample-collecting device would be a harpoonlike device that would be connected to the balloon-borne gondola by a tether long enough to reach the ground (see Figure 1). The device would be dropped from the gondola to acquire a sample, then would be reeled back up to the gondola, where the sample would be analyzed by the onboard instruments.

Each prototype of the sample-collecting device (see Figure 2) has a sharp front (lower) end, a hollow core for retaining a sample, a spring (not shown in the figure) for holding the sample in the hollow core, and a rear (upper) annular cavity for retaining liquid sample material. Aerodynamic fins at the rear help to keep the front end pointed downward. In tests, these prototype devices were dropped from various heights and used to gather samples of dry sand, moist sand, cryogenic water ice, and warmer water ice.

This work was done by Jack Jones, Wayne Zimmerman, and Jiunn Jenq Wu of Caltech for NASA's Jet Propulsion Laboratory. Further information is contained in a TSP (see page 1).
NPO-44444

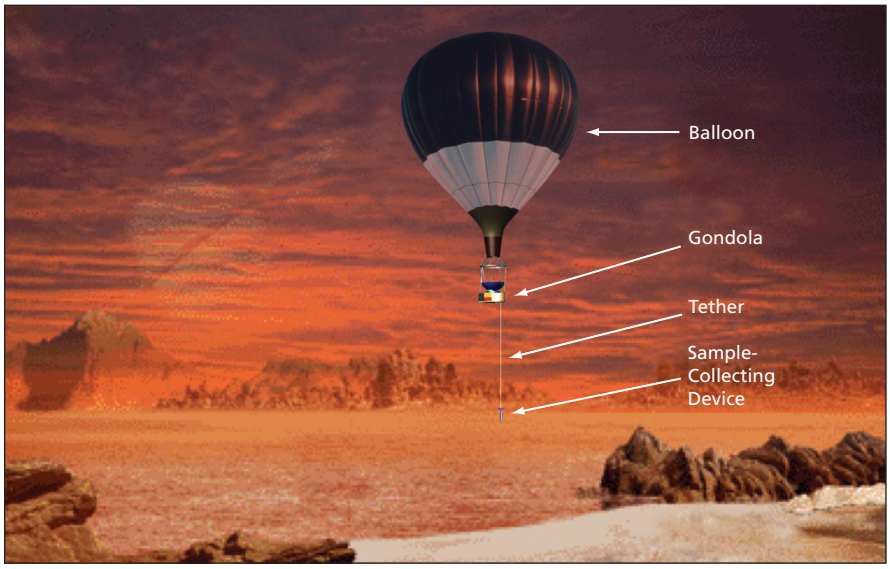

Figure 1. A **Tethered Sample-Collecting Device** would be dropped from a balloon-borne gondola to collect a sample of ground material, then reeled back up to the gondola to enable analysis of the sample.

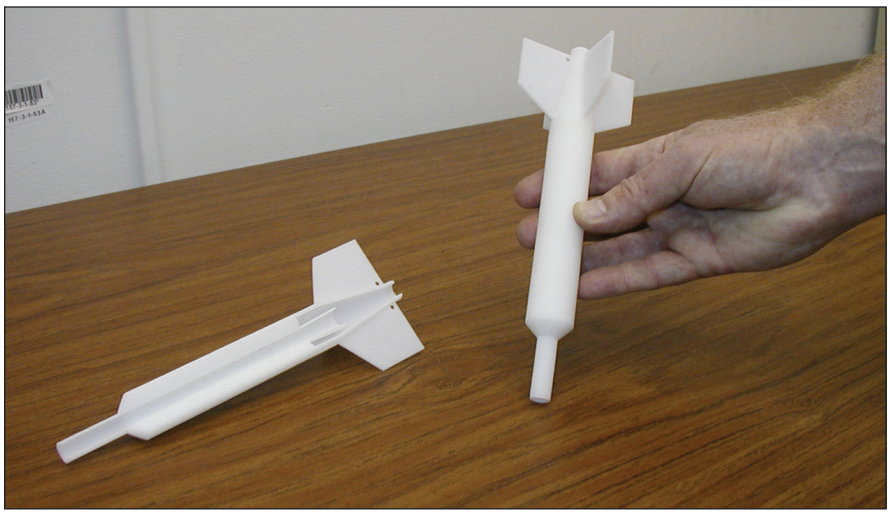

Figure 2. These **Prototype Sample-Collecting Devices** are basically harpoons with smooth, sharp front ends, rear stabilizing fins, and interior cavities for capturing and retaining samples.

Tethered Pyrotechnic Apparatus for Acquiring a Ground Sample

A tethered projectile would be pyrotechnically driven into the ground.

NASA's Jet Propulsion Laboratory, Pasadena, California

A proposed alternative design for the balloon-borne ground-sampling system described in the immediately preceding article would not rely on free fall to drive a harpoonlike sample-collecting device into the ground. Instead, the harpoon-like sample-collecting device would be a pyrotechnically driven, tethered projectile.

The apparatus would include a tripod that would be tethered to the gondola. A gun for shooting the projectile into the ground would be mounted at the apex of the tripod (see figure). The gun would include an electronic trigger circuit, a chamber at the breech end containing a pyrotechnic charge, and a barrel. A sabot would be placed in the

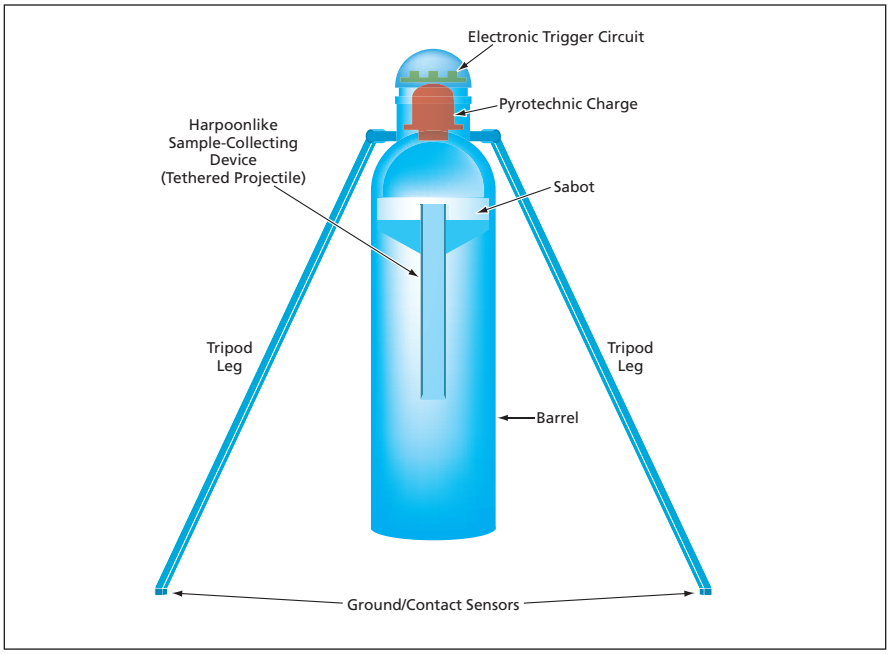

A **Gun Aimed Downward From the Top of a Tripod** would fire a tethered projectile into the ground to collect a sample when all three feet of the tripod simultaneously touch the ground.

barrel just below the pyrotechnic charge, and the tethered projectile would be placed in the barrel just below the sabot. The tripod feet would be equipped with contact sensors connected to the trigger circuit.

In operation, the tripod would be lowered to the ground on its tether. Once contact with the ground was detected by the sensors on all three tripod feet, the trigger circuit would fire the pyrotechnic charge to drive the projectile into the ground. (Requiring contact among all three tripod feet and the ground would ensure that the projectile would be fired into the ground, rather than up toward the gondola or the balloon.) The tethered projectile would then be reeled back up to the gondola for analysis of the sample.

This work was done by Jack Jones, Wayne Zimmerman, Jiunn Jenq Wu, Mircea Badescu, and Stewart Sherrit of Caltech for NASA's Jet Propulsion Laboratory. Further information is contained in a TSP (see page 1). ***NPO-44445***

Enhanced Video-Oculography System

Lyndon B. Johnson Space Center, Houston, Texas

A previously developed video-oculography system has been enhanced for use in measuring vestibulo-ocular reflexes of a human subject in a centrifuge, motor vehicle, or other setting. The system as previously developed included a lightweight digital video camera mounted on goggles. The left eye was illuminated by an infrared light-emitting diode via a dichroic mirror, and the camera captured images of the left eye in infrared light. To extract eye-movement data, the digitized video images were processed by software running in a laptop computer. Eye movements were calibrated by having the subject view a target pattern, fixed with respect to the subject's head, generated by a goggle-mounted laser with a diffraction grating.

The system as enhanced includes a second camera for imaging the scene from the subject's perspective, and two inertial measurement units (IMUs) for measuring linear accelerations and rates of rotation for computing head movements. One IMU is mounted on the goggles, the other on the centrifuge or vehicle frame. All eye-movement and head-motion data are time-stamped. In addition, the subject's point of regard is superimposed on each scene image to enable analysis of patterns of gaze in real time.

This work was done by Steven T. Moore and Hamish G. MacDougall of Mount Sinai School of Medicine for Johnson Space Center. For further information, contact the JSC Innovation Partnerships Office at (281) 483-3809. ***MSC-23957-1***

Joint Carrier-Phase Synchronization and LDPC Decoding

Soft feedback from an LDPC decoder would enhance performance of a PLL.

NASA's Jet Propulsion Laboratory, Pasadena, California

A method has been proposed to increase the degree of synchronization of a radio receiver with the phase of a suppressed carrier signal modulated with a binary-phase-shift-keying (BPSK) or quaternary-phase-shift-keying (QPSK) signal representing a low-density parity-check (LDPC) code. This method is an extended version of the method described in "Using LDPC Code Constraints to Aid Recovery of Symbol Timing" (NPO-43112), *NASA Tech Briefs*, Vol. 32, No. 10 (October 2008), page 54. Both methods and the receiver architectures in which they would be implemented belong to a class of timing-recovery methods and corresponding receiver architectures characterized as pilotless in that they do not require transmission and reception of pilot signals.

The proposed method calls for the use of what is known in the art as soft decision feedback to remove the modulation from a replica of the incoming signal prior to feeding this replica to a phase-locked loop (PLL) or other carrier-tracking stage in the receiver. "Soft decision feedback" refers to suitably processed versions of intermediate results of iterative computations involved in the LDPC decoding process. Unlike a related prior method in which hard decision feedback (the final sequence of decoded symbols) is used to remove the modulation, the proposed method does not require estimation of the decoder error probability.

In a basic digital implementation of the proposed method (see figure), the incoming signal (having carrier phase θ_c) plus noise would first be converted to in-phase (I) and quadrature (Q) baseband signals by mixing it with I and Q signals at the carrier frequency $[\omega_c/(2\pi)]$ generated by a local oscillator. The resulting demodulated signals would be processed through one-symbol-period integrate-and-dump filters, the outputs of which would be sampled and held, then multiplied by a soft-decision version of the baseband modulated signal. The resulting I and Q products consist of terms proportional to the cosine and sine of the carrier phase θ_c as well as correlated noise components. These products would be fed as inputs to a digital PLL that would include a number-controlled oscillator (NCO), which provides an estimate of the carrier phase, $\hat{\theta}_c$.

This work was done by Marvin Simon and Christopher Jones of Caltech and Esteban Valles of the University of California, Los Angeles, for NASA's Jet Propulsion Laboratory.

In accordance with Public Law 96-517, the contractor has elected to retain title to this invention. Inquiries concerning rights for its commercial use should be addressed to:

Innovative Technology Assets Management
JPL
Mail Stop 202-233
4800 Oak Grove Drive
Pasadena, CA 91109-8099
(818) 354-2240
E-mail: iaoffice@jpl.nasa.gov

Refer to NPO-43656, volume and number of this NASA Tech Briefs *issue, and the page number.*

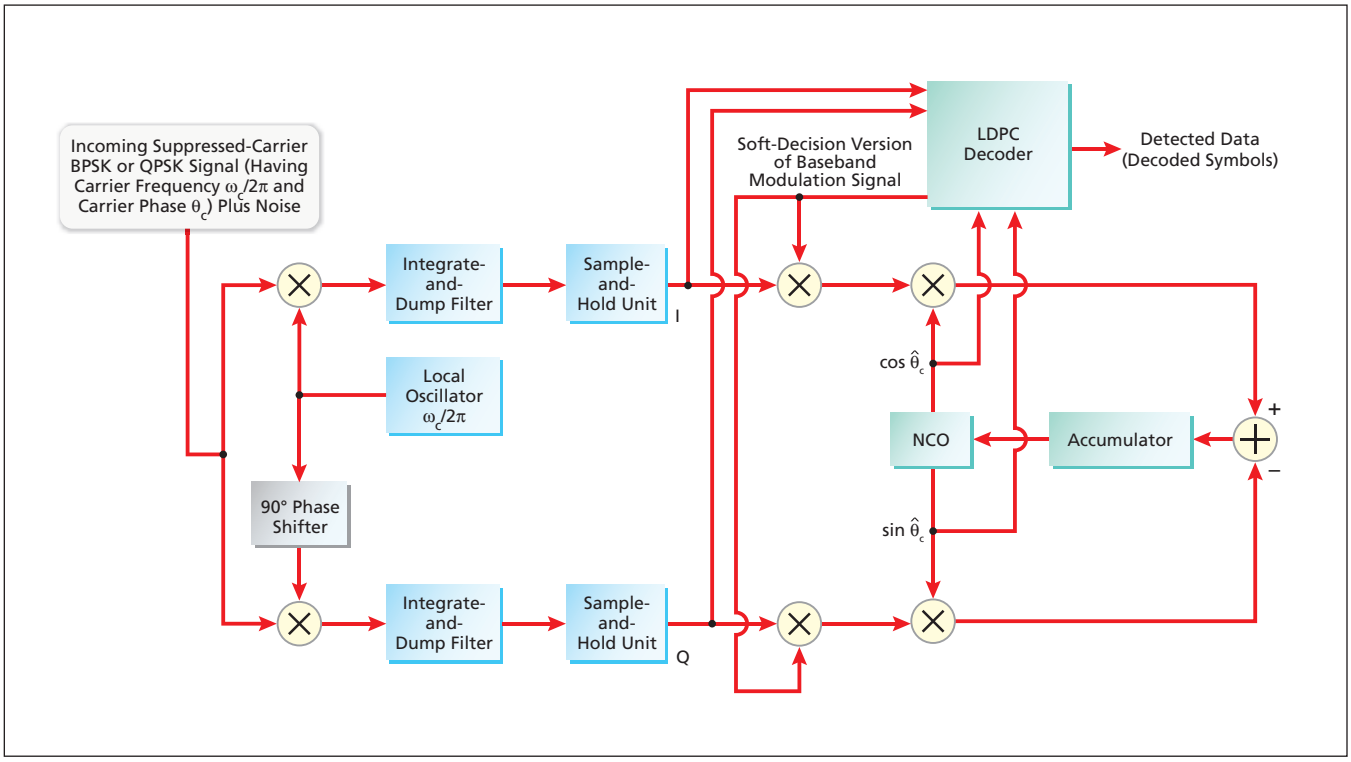

This **Digital Signal-Processing System** iteratively removes carrier phase modulation from the incoming suppressed carrier modulated signal.

Dual-Polarization, Sideband-Separating, Balanced Receiver for 1.5 THz

Development is enabled by recent advances in simulation and microfabrication.

NASA's Jet Propulsion Laboratory, Pasadena, California

A proposed heterodyne receiver would be capable of detecting electromagnetic radiation in both of two orthogonal linear polarizations, separating sidebands, and providing balanced outputs in a frequency band centered at 1.5 THz with a fractional bandwidth >40 percent. Dual-polarization, sideband-separating, and balanced-output receivers are well-known and have been used extensively at frequencies up to about 100 GHz; and there was an earlier proposal for such a receiver for frequencies up to 900 GHz. However, the present proposal represents the first realistic design concept for such a receiver capable of operating above 1 THz. The proposed receiver is intended to be a prototype of mass-producible receiver units, operating at frequencies up to 6 THz, that would be incorporated into highly sensitive heterodyne array instruments to be used in astronomical spectroscopic and imaging studies.

The receiver architecture (see Figure 1) as proposed is based on discrete single-ended mixers and conventional waveguides with integrated planar circuitry. The receiver would include a finline orthomode transducer (OMT) followed by six quadrature hybrids on a plane (see Figure 2). An incoming radio-frequency (RF) signal would enter via a horn antenna. An orthomode transducer (OMT) would separate the incoming RF signal into its two orthogonal linearly polarized components. One of the outputs will go through a waveguide polarization twist and that will enable the subsequent components to have the same E-field orientation. Each of these polarizations would be fed to a first-stage quadrature hybrid. The outputs of each first-stage quadrature hybrid, which would be in phase quadrature, would be fed along with a local-oscillator (LO) signal to two second-stage quadrature hybrids. The combined LO and RF signals coming out of the second-stage quadrature hybrids would pump two sets of mixers in a balanced configuration. The intermediate-frequency (IF) outputs of the mixers would be combined in third-stage quadrature hybrids to separate the upper and lower sidebands for each polarization.

The critical components in the planned development of the proposed receiver would be the OMT, the first- and second-stage quadrature hybrids, and the polarization twist. Previously, it was almost impossible to design, simulate, and fabricate such components for operation at terahertz frequencies:

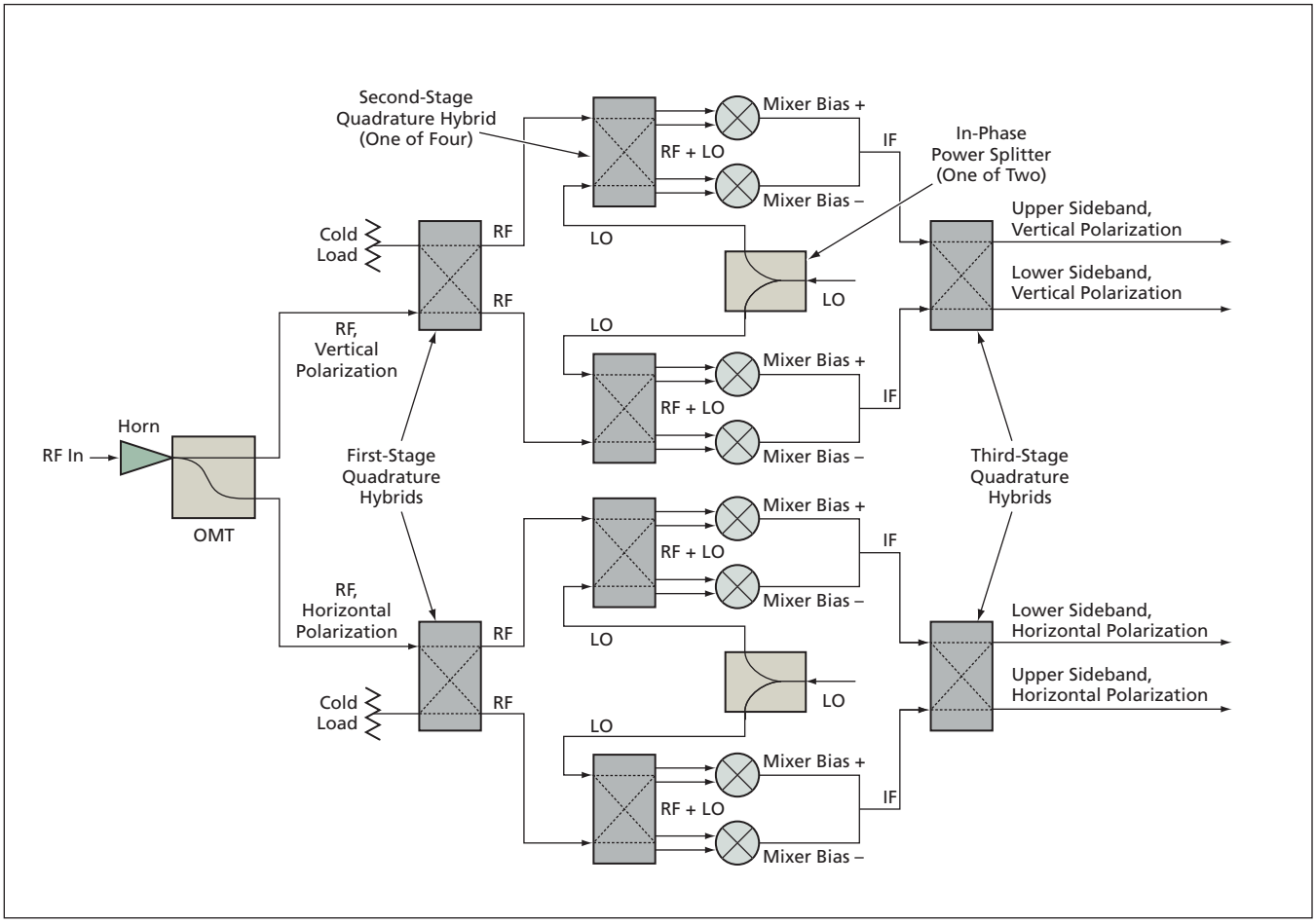

Figure 1. The **1.5-THz Dual-Polarization, Sideband-Separating Receiver** would process an incoming RF signal into an upper- and a lower-sideband output for each of two orthogonal polarizations.

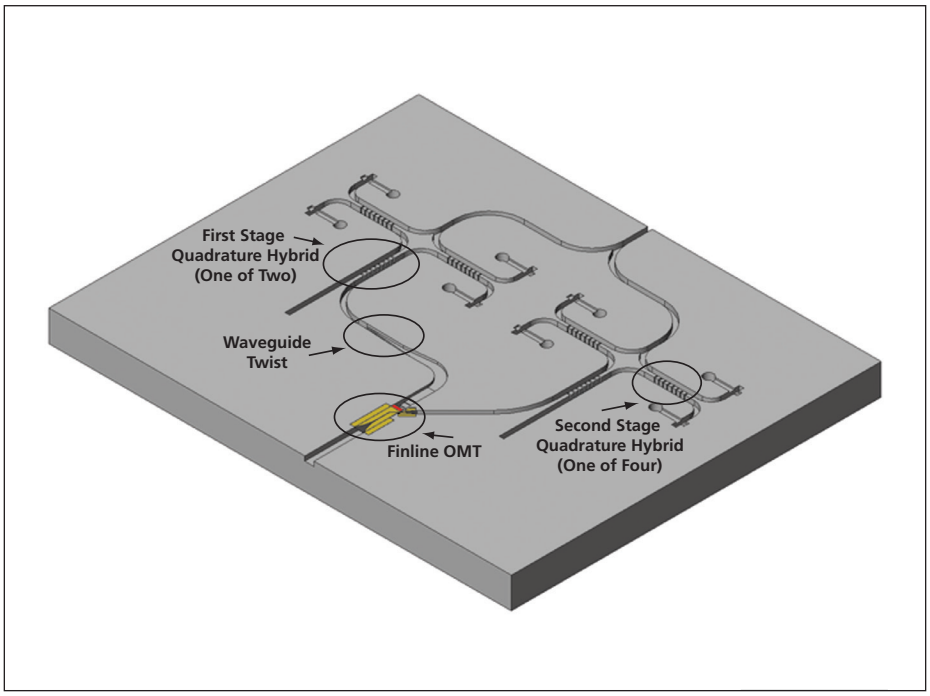

Figure. 2. A schematic diagram of the **One Half of the Split-Block** for the broadband 1.5 THz dual-polarized, sideband-separating, balanced receiver shows the finline OMT, two first-stage and four second-stage quadrature hybrids, and the in-phase LO power splitter that will be fabricated using DRIE silicon etching process.

because of the smallness of their features and the tightness of their tolerances, quadrature hybrids and finline OMTs for terahertz frequencies cannot be fabricated by conventional machining. However, recent advances in both electromagnetic-field-simulating software and microfabrication techniques have made it possible to design and construct complexly shaped waveguide structures. The development of the proposed receiver is planned to include the use of a combination of optical lithography and a micromachining process based on deep reactive ion etching (DRIE) of silicon. This combination is expected to enable the realization of micron-size waveguide features and sub-micron tolerances in fabricating the aforementioned critical components.

This work was done by Goutam Chattopadhyay, John Ward, Harish Manohara, and Peter Siegel of Caltech for NASA's Jet Propulsion Laboratory.

In accordance with Public Law 96-517, the contractor has elected to retain title to this invention. Inquiries concerning rights for its commercial use should be addressed to:

Innovative Technology Assets Management
JPL
Mail Stop 202-233
4800 Oak Grove Drive
Pasadena, CA 91109-8099
(818) 354-2240
E-mail: iaoffice@jpl.nasa.gov

Refer to NPO-42935, volume and number of this NASA Tech Briefs *issue, and the page number.*

Modular Battery Charge Controller

Distributed charge control and a masterless communication bus enhance this controller's robustness for use in battery energy-storage applications.

John H. Glenn Research Center, Cleveland, Ohio

A new approach to masterless, distributed, digital-charge control for batteries requiring charge control has been developed and implemented. This approach is required in battery chemistries that need cell-level charge control for safety and is characterized by the use of one controller per cell, resulting in redundant sensors for critical components, such as voltage, temperature, and current. The charge controllers in a given battery interact in a masterless fashion for the purpose of cell balancing, charge control, and state-of-charge estimation. This makes the battery system invariably fault-tolerant.

The solution to the single-fault failure, due to the use of a single charge controller (CC), was solved by implementing one CC per cell and linking them via an isolated communication bus [e.g., controller area network (CAN)] in a masterless fashion so that the failure of one or more CCs will not impact the remaining functional CCs. Each microcontroller-based CC digitizes the cell voltage (V_{cell}), two cell temperatures, and the voltage across the switch (V); the latter variable is used in conjunction with V_{cell} to estimate the bypass current for a given bypass resistor. Furthermore, CC1 digitizes the battery current (I_1) and battery voltage (V_{batt}) and CC5 digitizes a second battery current (I_2). As a result, redundant readings are taken for temperature, battery current, and battery voltage through the summation of the individual cell voltages given that each CC knows the voltage of the other cells.

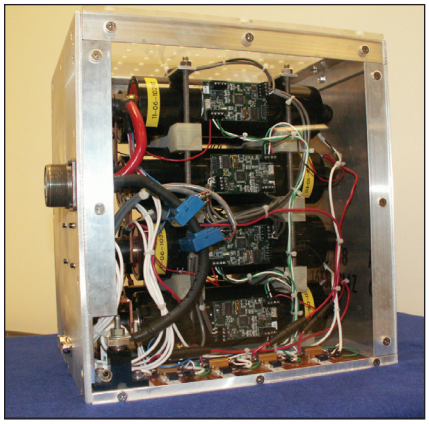

A prototype of the 28-V, 60-A-h **Lithium Ion Battery**.

For the purpose of cell balancing, each CC periodically and independently transmits its cell voltage and stores the

received cell voltage of the other cells in an array. The position in the array depends on the identifier (ID) of the transmitting CC. After eight cell voltage receptions, the array is checked to see if one or more cells did not transmit. If one or more transmissions are missing, the missing cell(s) is (are) eliminated from cell-balancing calculations.

The cell-balancing algorithm is based on the error between the cell's voltage and the other cells and is categorized into four zones of operation. The algorithm is executed every second and, if cell balancing is activated, the error variable is set to a negative low value. The largest error between the cell and the other cells is found and the zone of operation determined. If the error is zero or negative, then the cell is at the lowest voltage and no balancing action is needed. If the error is less than a predetermined negative value, a Cell Bad Flag is set. If the error is positive, then cell balancing is needed, but a hysteretic zone is added to prevent the bypass circuit from triggering repeatedly near zero error. This approach keeps the cells within a predetermined voltage range.

This work was done by Robert Button of Glenn Research Center and Marcelo Gonzalez of Cleveland State University. Further information is contained in a TSP (see page 1).

Inquiries concerning rights for the commercial use of this invention should be addressed to NASA Glenn Research Center, Innovative Partnerships Office, Attn: Steve Fedor, Mail Stop 4–8, 21000 Brookpark Road, Cleveland, Ohio 44135. Refer to LEW-18296-1.

Efficient Multiplexer FPGA Block Structures Based on G^{4}FETs

Fewer G^{4}FETs than conventional transistors would be needed to implement multiplexers.

NASA's Jet Propulsion Laboratory, Pasadena, California

Generic structures have been conceived for multiplexer blocks to be implemented in field-programmable gate arrays (FPGAs) based on four-gate field-effect transistors (G^{4}FETs). This concept is a contribution to the continuing development of digital logic circuits based on G^{4}FETs and serves as a further demonstration that logic circuits based on G^{4}FETs could be more efficient (in the sense that they could contain fewer transistors), relative to functionally equivalent logic circuits based on conventional transistors.

Results in this line of development at earlier stages were summarized in two previous *NASA Tech Briefs* articles: "G^{4}FETs as Universal and Programmable Logic Gates" (NPO-41698), Vol. 31, No. 7 (July 2007), page 44, and "Efficient G^{4}FET-Based Logic Circuits" (NPO-44407), Vol. 32, No. 1 (January 2008), page 38 . As described in the first-mentioned previous article, a G^{4}FET can be made to function as a three-input NOT-majority gate, which has been shown to be a universal and programmable logic gate. The universality and programmability could be exploited to design logic circuits containing fewer components than are required for conventional transistor-based circuits performing the same logic functions. The second-mentioned previous article reported results of a comparative study of NOT-majority-gate

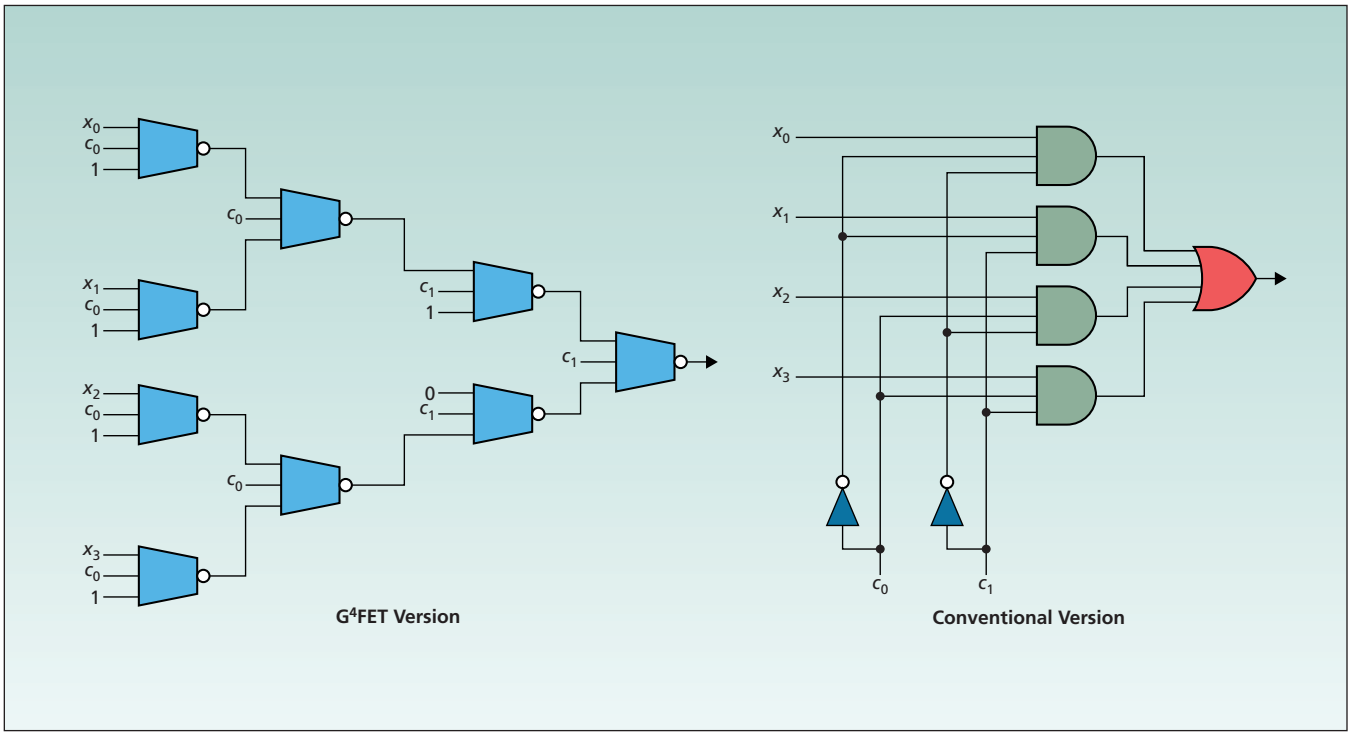

A **Four-to-One Multiplexer** is a special case of a 2^n-to-1 multiplexer, which can perform a variety of logic functions on 2^n binary data inputs ($x_0,...x_{2^n-1}$), and n control (selection) inputs ($c_0,...c_{n-1}$). In this case, n = 2. The combination of the control inputs can be interpreted as a binary integer, c, in the range of 0 to $2^n - 1$.

(G^4FET)-based logic-circuit designs and equivalent NOR- and NAND-gate-based designs utilizing conventional transistors. [NOT gates (inverters) were also included, as needed, in both the G^4FET- and the NOR- and NAND-based designs.] In most of the cases studied, fewer logic gates (and, hence, fewer transistors), were required in the G^4FET-based designs.

There are two popular categories of FPGA block structures or architectures: one based on multiplexers, the other based on lookup tables. In standard multiplexer-based architectures, the basic building block is a treelike configuration of multiplexers, with possibly a few additional logic gates such as ANDs or ORs. Interconnections are realized by means of programmable switches that may connect the input terminals of a block to output terminals of other blocks, may bridge together some of the inputs, or may connect some of the input terminals to signal sources representing constant logical levels 0 or 1.

The left part of the figure depicts a four-to-one G^4FET-based multiplexer tree; the right part of the figure depicts a functionally equivalent four-to-one multiplexer based on conventional transistors. The G^4FET version would contains 54 transistors; the conventional version contains 70 transistors.

This work was done by Farrokh Vatan and Amir Fijany of Caltech for NASA's Jet Propulsion Laboratory. Further information is contained in a TSP (see page 1).

In accordance with Public Law 96-517, the contractor has elected to retain title to this invention. Inquiries concerning rights for its commercial use should be addressed to:

Innovative Technology Assets Management
JPL
Mail Stop 202-233
4800 Oak Grove Drive
Pasadena, CA 91109-8099
E-mail: iaoffice@jpl.nasa.gov

Refer to NPO-44735, volume and number of this NASA Tech Briefs *issue, and the page number.*

VLSI Microsystem for Rapid Bioinformatic Pattern Recognition

Rapid processing is made possible by a massively parallel neural-computing architecture.

NASA's Jet Propulsion Laboratory, Pasadena, California

A system comprising very-large-scale integrated (VLSI) circuits is being developed as a means of bioinformatics-oriented analysis and recognition of patterns of fluorescence generated in a microarray in an advanced, highly miniaturized, portable genetic-expression-assay instrument. Such an instrument implements an on-chip combination of polymerase chain reactions and electrochemical transduction for amplification and detection of deoxyribonucleic acid (DNA).

Commonly, the design of such an instrument provides for a sample and a reference channel, so that it can be used to perform a dual-label assay for identifying differentially expressed genes. A dual-label assay also reduces spurious variability attributable to aspects of spots in the microarray that affect both the sample and the reference specimen similarly. The logarithm of the relative intensities of the two fluorescent-dye-labeled specimens at each spot is calculated and used in analyzing the fluorescence image of the assay. Heretofore, analysis of the fluorescence image has typically involved sequential, pixel-by-pixel processing in a digital computer. Such processing does not enable real-time recognition of genetic patterns of interest — a significant drawback where, for example, it may be desirable or necessary to recognize dangerous microbes in the field. In contrast, a system like the one now being developed enables robust, real-time recognition.

The system (see figure) includes a chip, denoted a biochip, that contains VLSI circuitry for collecting the fluorescence inputs and generates analog signals proportional to the logarithms of the fluorescence-intensity ratios for the spots in the microarray. The outputs of the biochip are fed as inputs to another chip that contains a VLSI artificial neural network (ANN), which performs the processing for recognition of bioinformatic patterns of interest. The ANN design pro-

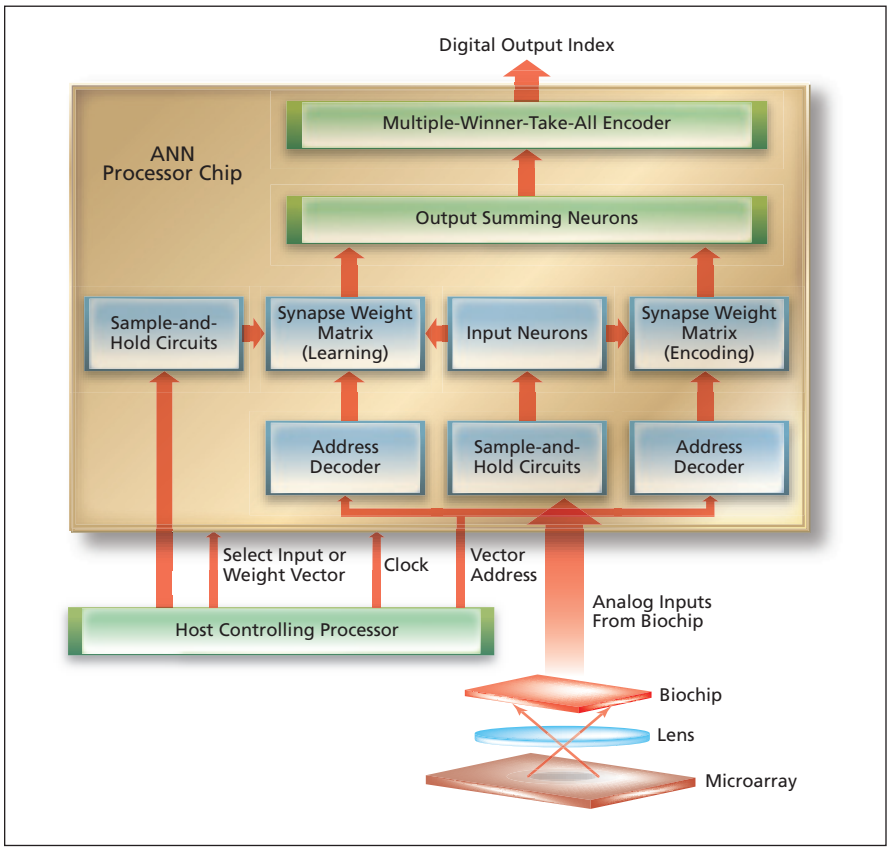

The **Biochip Collects Fluorescence Inputs** from the microarray and feeds them to the ANN processor chip, which strives to recognize a bioinformatic pattern of interest.

vides for a combination of massively parallel neural-computing interconnections and mixed-signal (a combination of analog and digital) circuitry characterized by feature sizes in the deep-submicron range, making it possible to implement the ANN as a single VLSI chip. One notable aspect of the design is the use of a parallel row/column data-flow architecture to connect all on-chip subsystems and eliminate data-flow bottlenecks of the type caused by bandwidth limitations in conventional data buses.

The ANN includes input neurons, programmable-weight synapses, summing and inner product cells, output neurons, and an output multi-winner-take-all encoder. The programmable synapse matrix is composed of $M \times N$ cells for $N \times M$-dimensional code vectors. There are N output summing neurons that execute a sigmoid-logarithmic (in contradistinction to a conventional sigmoid) transfer function. The synaptic weights are generated by an error-back-propagation supervised-learning algorithm executed by an off-chip host controlling processor. The outputs of the output summing neurons are fed to a multi-winner-take-all block that consists of N competitive circuit cells and uses binary codes to encode N classes.

This work was done by Wai-Chi Fang of Caltech and Jaw-Chyng Lue of University of Southen California for NASA's Jet Propulsion Laboratory. Further information is contained in a TSP (see page 1).

In accordance with Public Law 96-517, the contractor has elected to retain title to this invention. Inquiries concerning rights for its commercial use should be addressed to:

Innovative Technology Assets Management
JPL
Mail Stop 202-233
4800 Oak Grove Drive
Pasadena, CA 91109-8099
(818) 354-2240
E-mail: iaoffice@jpl.nasa.gov

Refer to NPO-44155, volume and number of this NASA Tech Briefs *issue, and the page number.*

Low-Noise Amplifier for 100 to 180 GHz

Noise temperature is lower than in the prior state of the art.

NASA's Jet Propulsion Laboratory, Pasadena, California

A three-stage monolithic millimeter-wave integrated-circuit (MMIC) amplifier designed to exhibit low noise in operation at frequencies from about 100 to somewhat above 180 GHz has been built and tested. This is a prototype of broadband amplifiers that have potential utility in diverse applications, including measurement of atmospheric temperature and humidity and millimeter-wave imaging for inspecting contents of opaque containers.

Figure 1 depicts the amplifier as it appears before packaging. Figure 2 presents data from measurements of the performance of the amplifier as packaged in a WR-05 waveguide and tested in the frequency range from about 150 to about 190 GHz. The amplifier exhibited substantial gain throughout this frequency range. Especially notable is the fact that at 165 GHz, the noise figure was found to be 3.7 dB, and the noise temperature was found to be 370 K: This is less than half the noise temperature of the prior state of the art.

This work was done by Pekka Kangaslahti, David Pukala, King Man Fung, and Todd Gaier of Caltech and Xiaobing Mei, Richard Lai, and William Deal of Northrop Grumman Corporation for NASA's Jet Propulsion Laboratory. For more information, contact iaoffice@jpl.nasa.gov. NPO-45178

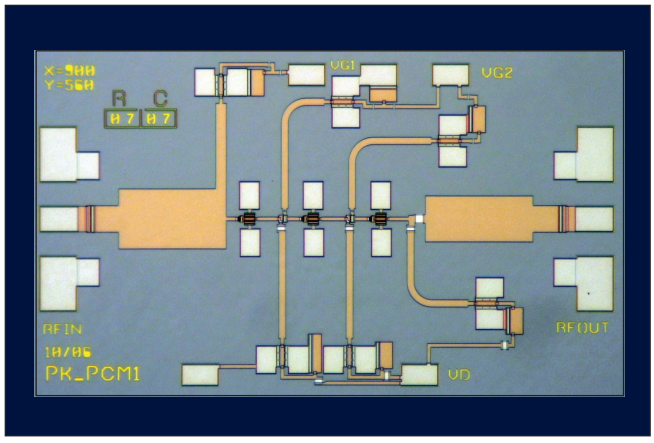

Figure 1. This **MMIC Amplifier** includes InP high-electron-mobility transistors (HEMTs) connected to microstrip transmission lines on a substrate of 2-mil (≈51-μm) thickness. Each HEMT has two fingers and a gate width of 15 μm, for a total gate periphery of 30 μm.

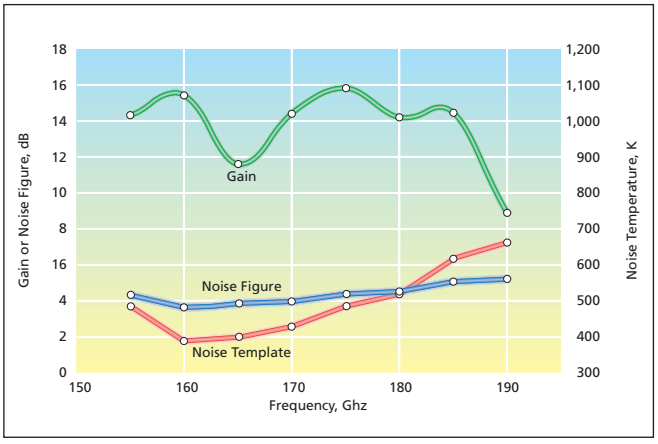

Figure 2. These **Plots of Performance Data** were derived from measurements on the amplifier as packaged in a WR-05 waveguide [a waveguide having a cross section of 0.0510 by 0.0255 in. (about 1.30 by 0.65 mm), nominally for the frequency range of 140 to 220 GHz].

Improved Fabrication of Ceramic Matrix Composite/Foam Core Integrated Structures

CMC face sheets bonded to ceramic foam cores are delamination-resistant and reduce cost, weight, and maintenance.

John H. Glenn Research Center, Cleveland, Ohio

The use of hybridized carbon/silicon carbide (C/SiC) fabric to reinforce ceramic matrix composite face sheets and the integration of such face sheets with a foam core creates a sandwich structure capable of withstanding high-heat-flux environments (150 W/cm^2) in which the core provides a temperature drop of 1,000 °C between the surface and the back face without cracking or delamination of the structure. The composite face sheet exhibits a bilinear response, which results from the SiC matrix not being cracked on fabrication. In addition, the structure exhibits damage tolerance under impact with projectiles, showing no penetration to the back face sheet. These attributes make the composite ideal for leading-edge structures and control surfaces in aerospace vehicles, as well as for acreage thermal protection systems and in high-temperature, lightweight stiffened structures.

By tailoring the coefficient of thermal expansion (CTE) of a carbon fiber-containing ceramic matrix composite (CMC) face sheet to match that of a ceramic foam core, the face sheet and the core can be integrally fabricated without any delamination. Carbon and SiC are woven together in the reinforcing fabric. Integral densification of the CMC and the foam core is accomplished with chemical vapor deposition, eliminating the need for bond-line adhesive. This means there is no need to separately fabricate the core and the face sheet, or to bond the two elements together, risking edge delamination during use.

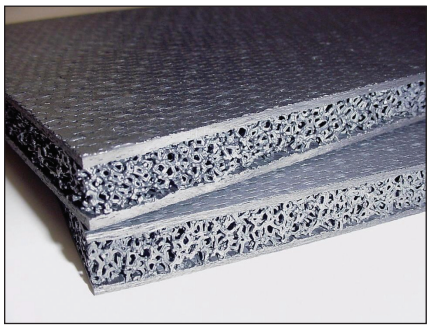

The **Foam Core Ceramic Matrix Composite** is a weave SiC and carbon fiber, which allows heat dissipation in-plane. Face sheet thickness is nominally 2.4 mm, and core thickness is 1.26 cm.

Fibers of two or more types are woven together on a loom. The carbon and ceramic fibers are pulled into the same "pick" location during the weaving process. Tow spacing may be varied to accommodate the increased volume of the combined fiber tows while maintaining a target fiber volume fraction in the composite. Foam pore size, strut thickness, and ratio of face sheet to core thickness can be used to tailor thermal and mechanical properties. The anticipated CTE for the hybridized composite is managed by the choice of constituents, varying fiber tow sizes and constituent part ratios.

This structural concept provides high strength and stiffness at low density — 1.06 g/cm^3 in panels tested. Varieties of face sheet constructions are possible, including variations in fiber type and weave geometry. The integrated structures possible with this composite could eliminate the need for non-load-bearing thermal protection systems on top of a structural component. The back sheet can readily be integrated to substructures through the incorporation of ribs. This would eliminate weight and cost for aerospace missions.

This work was done by Frances I. Hurwitz of Glenn Research Center. Further information is contained in a TSP (see page 1).

Inquiries concerning rights for the commercial use of this invention should be addressed to NASA Glenn Research Center, Innovative Partnerships Office, Attn: Steve Fedor, Mail Stop 4–8, 21000 Brookpark Road, Cleveland, Ohio 44135. Refer to LEW-18126-1.

Inert Welding/Brazing Gas Filters and Dryers

This system can be used in any process requiring reduction of inert-gas moisture level.

John F. Kennedy Space Center, Florida

A system has been designed to reduce the hydrogen molecule content in inert gases that are used for shielding the welding arc and molten weld area during the manual fusion, automated welding, and induction brazing process. Two desiccant pipeline dryer cartridges are connected together using either aircraft or KC .250 fittings, and are installed in-line between the inert-gas facility source (argon and helium) and the welding machine. This process helps maintain alloy grain structure and integrity to engineering specifications during the welding and brazing processes. Also, this method enhances weldability when joining similar and dissimilar alloys. It is easy to restore the system to original drying capabilities by using a nitrogen purge or by oven drying. This design has low schedule impact or down time when being installed on machines or in systems. There is also a sight glass to indicate when servicing is needed.

Reducing the moisture level in ultra-high-purity gasses also lowers costs. The

total cost of the system described here was less than $1,000 (at the time of this reporting). It has been in operation for 4.5 years with no maintenance or drying. The last test of the system indicated the gas moisture level was less than 2 ppm, with a dew point of less than –97 °F (–72 °C). Before the line dryers were installed, the inlet gases had a moisture rating of 15 ppm. With the installation of a one-canister system, the inert gas moisture level dropped to 3 ppm. When a two-canister system was installed, the inert gas moisture level dropped to 0.7 ppm.

These two pipeline dryers also act as a mixing chamber for both argon and helium gases, which is crucial for applications of certain critical welding processes. This innovation is applicable to any process or system that requires a reduction of any inert gas moisture level (in ppm). It may also be used in any process or system, such as avionics, that uses inert gases with a low moisture level requirement of 1 ppm or lower, depending on the cubic feet per minute (CFM) flow rate.

This work was done by Jerry Goudy of United Space Alliance for Kennedy Space Center. Further information is contained in a TSP (see page 1). ***KSC-13189***

Fabricating Copper Nanotubes by Electrodeposition

Relative to copper nanorods, copper nanotubes can be fabricated at lower cost.

NASA's Jet Propulsion Laboratory, Pasadena, California

Copper tubes having diameters between about 100 and about 200 nm have been fabricated by electrodeposition of copper into the pores of alumina nanopore membranes. Copper nanotubes are under consideration as alternatives to copper nanorods and nanowires for applications involving thermal and/or electrical contacts, wherein the greater specific areas of nanotubes could afford lower effective thermal and/or electrical resistivities. Heretofore, copper nanorods and nanowires have been fabricated by a combination of electrodeposition and a conventional expensive lithographic process. The present electrodeposition-based process for fabricating copper nanotubes costs less and enables production of copper nanotubes at greater rate.

The demonstration of this process began with the selection of alumina membranes containing pores having diameters in the approximate range of 100 to 200 nm. The estimated porosity of these membranes was 43 percent. Each of these membranes was evaporation-coated on one side with a 100-nm-thick gold film to render that side electrically conductive. Each membrane was then mounted on a gold-coated silicon substrate by use of adhesive tape, and the substrate was carefully masked with tape to prevent electrodeposition on the substrate. Next, the membrane-and-substrate unit was immersed for about 10 minutes in a solution comprising 4 volume parts of water and 1 volume part of a potassium-based, buffered developer solution commonly used in lithography. The purpose and effect of this immersion was to render the surfaces of the pores electrically conductive.

Next, electrodeposition into the pores was performed at room temperature in a commercially available copper-plating solution, using platinum-coated titanium mesh counter electrodes and galvanostatic control set to a current density of, variously, 10 or 20 mA/cm^2. Copper nanotubes were thus formed in the pores at a deposition rate of 100 nm/min at the current density of 10 mA/cm^2 or 150 nm/min at the current density of 20 mA/cm^2.

This work was done by E. H. Yang, Christopher Ramsey, Youngsam Bae, and Daniel Choi of Caltech for NASA's Jet Propulsion Laboratory.

This invention is owned by NASA, and a patent application has been filed. Inquiries concerning nonexclusive or exclusive license for its commercial development should be addressed to the Patent Counsel, NASA Management Office–JPL. Refer to NPO-42261.

Reducing Aerodynamic Drag on Empty Open Cargo Vehicles

Open cargo bays are subdivided by means of simple partitions.

Ames Research Center, Moffett Field, California

Some simple structural modifications have been demonstrated to be effective in reducing aerodynamic drag on vehicles that have empty open cargo bays. The modifications were originally intended to be made in railroad coal cars because the amounts of coal and the distances over which they are transported by railroad in the United States are so large that the resulting reduction in drag could, potentially, result in an annual saving of millions of gallons of diesel fuel.

The basic idea is to break up the airflow in a large open cargo bay by inserting panels to divide the bay into a series of smaller bays. In the case of a coal car, this involves inserting a small number (typically between two and four) of vertical full-depth or partial-depth panels. For example, as shown in Figure 1, two triangular partial-depth vertical panels can be conveniently attached to triangular braces that are already integral parts of a typical coal car.

In an experiment, measurements of aerodynamic drag on models of coal cars were made in a wind tunnel. The results of the measurements, summarized in Figure 2, clearly show the drag-reducing effects of the dividers; they also show that the braces also contribute small reductions of drag.

This work was done by James C. Ross of Ames Research Center, Bruce L. Storms of AerospaceComputing, Inc., and Dan Dzoan of Ohlone College.

Inquiries concerning rights for the commercial use of this invention should be addressed to the Ames Technology Partnerships Division at (650) 604-2954. Refer to ARC-15422-1.

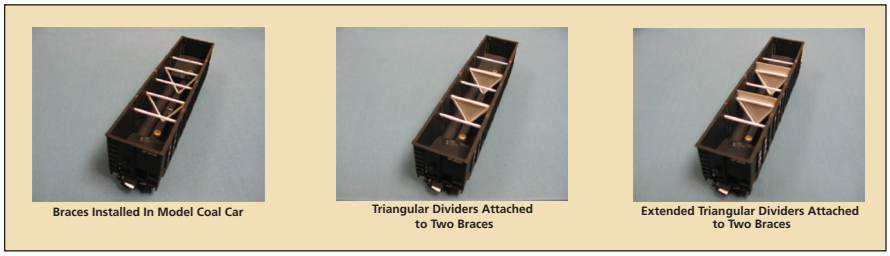

Figure 1. **Triangular Dividers** can be attached to triangular braces in a typical coal car to reduce aerodynamic drag when the car is empty.

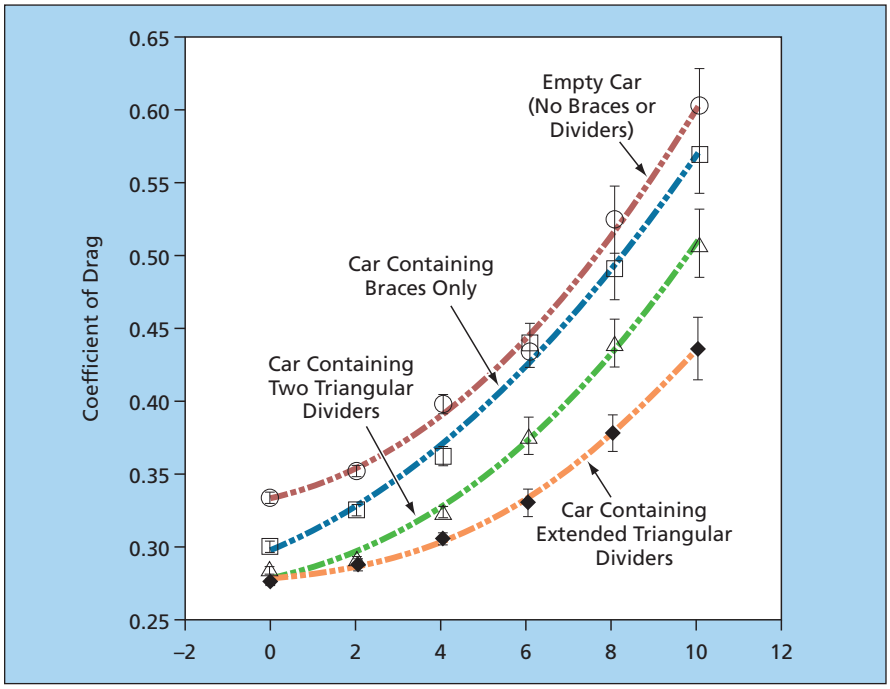

Figure 2. **Wind-Averaged Data** on the coefficient of drag were obtained in wind-tunnel tests of coal-car models like those of Figure 1. The yaw angle is the angle between the relative wind and the longitudinal axis of a car.

Rotary Percussive Auto-Gopher for Deep Drilling and Sampling

A drilling/sampling apparatus braces itself against the side of the hole.

NASA's Jet Propulsion Laboratory, Pasadena, California

The term "rotary percussive auto-gopher" denotes a proposed addition to a family of apparatuses, based on ultrasonic/sonic drill corers (USDCs), that have been described in numerous previous *NASA Tech Briefs* articles. These apparatuses have been designed, variously, for boring into, and/or acquiring samples of, rock or other hard, brittle materials of geological interest. In the case of the rotary percussive auto-gopher, the emphasis would be on developing an apparatus capable of penetrating to, and acquiring samples at, depths that could otherwise be reached

only by use of much longer, heavier, conventional drilling-and-sampling apparatuses.

To recapitulate from the prior articles about USDCs: A USDC can be characterized as a lightweight, low-power jackhammer in which a piezoelectrically driven actuator generates ultrasonic vibrations and is coupled to a tool bit through a free mass. The bouncing of the free mass between the actuator horn and the drill bit converts the actuator ultrasonic vibrations into sonic hammering of the drill bit. The combination of ultrasonic and sonic vibrations gives rise to a hammering action (and a resulting chiseling action at the tip of the tool bit) that is more effective for drilling than is the microhammering action of ultrasonic vibrations alone. The hammering and chiseling actions are so effective that the size of the axial force needed to make the tool bit advance into soil, rock, or another material of interest is much smaller than in ordinary rotary drilling, ordinary hammering, or ordinary steady pushing.

The predecessor of the rotary percussive auto-gopher is an apparatus, now denoted an ultrasonic/sonic gopher and previously denoted an ultrasonic gopher, described in "Ultrasonic/Sonic Mechanism for Drilling and Coring" (NPO-30291), *NASA Tech Briefs* Vol. 27, No. 9 (September 2003), page 65. The ultrasonic/sonic gopher is intended for use mainly in acquiring cores. The name of the apparatus reflects the fact that, like a gopher, it periodically stops advancing at the end of the hole to bring excavated material (in this case, a core sample) to the surface, then re-enters the hole to resume the advance of the end of the hole. By use of a cable suspended from a reel on the surface, the gopher is lifted from the hole to remove a core sample, then lowered into the hole to resume the advance and acquire the next core sample.

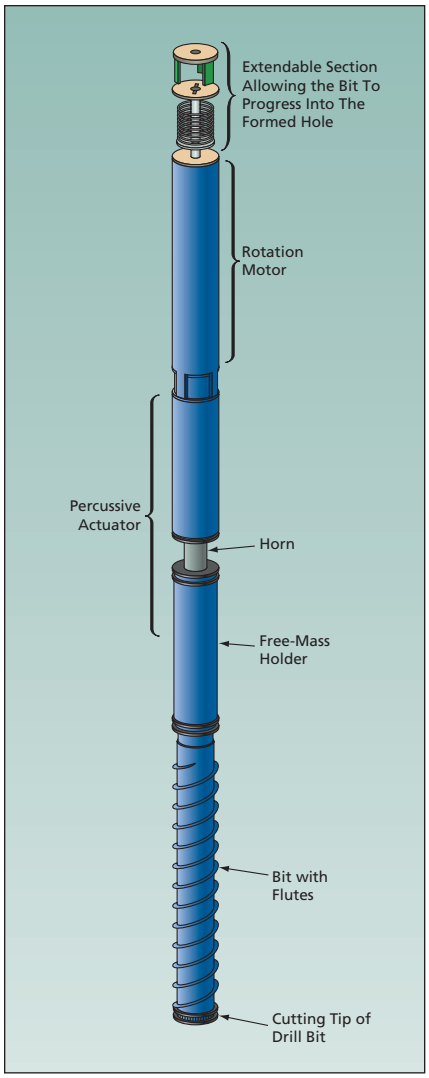

Anchoring and Rotary Mechanisms and a fluted drill bit would be added to an ultrasonic/sonic gopher.

The rotary percussive auto-gopher would include an ultrasonic/sonic gopher, to which would be added an anchoring and a rotary mechanism and a fluted drill bit (see figure). If, as intended, the ultrasonic/sonic gopher were rotated, then as in the case of an ordinary twist drill bit, the flutes would remove cuttings from the end of the hole, thereby making it possible to drill much faster than would be possible by ultrasonic/sonic hammering and chiseling action alone. The anchoring mechanism would brace itself against the wall of the drilled hole to enable the rotary mechanism to apply a small torque and a small axial preload to rotate the ultrasonic/sonic gopher drill bit and push the drill bit against the end of the hole. The anchoring and rotary mechanisms would be parts of an assembly that would follow the ultrasonic/sonic gopher down the hole.

This work was done by Yoseph Bar-Cohen, Mircea Badescu, and Stewart Sherrit of Caltech for NASA's Jet Propulsion Laboratory. Further information is contained in a TSP (see page 1). ***NPO-45949***

More About Reconfigurable Exploratory Robotic Vehicles

Essential to reconfigurability is modularity of hardware and software.

NASA's Jet Propulsion Laboratory, Pasadena, California

Modular exploratory robotic vehicles that will be able to reconfigure themselves in the field are undergoing development. These vehicles at the initial concept stage were described in "Reconfigurable Exploratory Robotic Vehicles" (NPO-20944), *NASA Tech Briefs*, Vol. 25, No. 7 (July 2001), page 56. Proposed for use in exploration of the surfaces of Mars and other remote planets, these vehicles and others of similar design could also be useful for exploring hostile terrain on Earth.

To recapitulate from the cited prior article: the modular vehicles are denoted generally by the term Axel*n*, where *n* is an even number equal to the number of main wheels. The simplest vehicle of this type is Axel2 — a two-main-wheel module that superficially resembles the rear axle plus rear wheels of an automobile (see Figure 1). In addition to the two main wheels, an Axel2 includes a passive caster wheel attached to the axle by an actuated caster link. The motion of the caster link can be used to control the rotation of the axle in order to tilt, to the desired angle, any sensors mounted on the axle. In addition to the sensors, the axle of an Axel2 houses computer modules and three motors and associated mechanisms for driving the main wheels and the caster link. An Axel2 is powered by rechargeable batteries located inside the wheel hubs.

One constructs an Axel*n* ($n > 2$) as an assembly of multiple Axel2s plus one or more instrument module(s) connected to each other at module interfaces (see Figure 2). The module interfaces contain standardized electrical and mechanical connections, including spring-loaded universal joints that afford some compliance to enable the modules to rotate, relative to each other, to adapt to

terrain. Data are communicated between modules via fast serial links in the module interfaces.

An Axel*n* amounts to a train carrying $n/2 - 1$ instrument modules. The instrument modules contain additional computational units that, in addition to processing of instrument readings, contribute to coordination of motion. In other words, the "intelligence" of an Axel*n*, and thus the sophistication of the maneuvers that it can perform, increase with *n*. The symmetrical design of the modules enables them to operate in any stable orientation, including upsidedown; this feature contributes to robustness of operation in rough terrain. A fully developed Axel*n* would be able to diagnose itself to detect nonfunctional modules.

Going beyond the description in the cited prior article, the following additional major items of the hardware can now be reported.

Also contained within the axle of an Axel2 is a stereoscopic pair of electronic cameras to be used for navigation across terrain, for scientific observations, and for guidance in docking maneuvers.

Each module interface is an electromechanical module located at the midlength of the axle of an Axel2. The module interface carries female parts of mating mechanisms, while instrument modules carry the male parts. The mating mechanisms include conical mating surfaces that correct for small initial misalignments to facilitate autonomous coupling of an Axel2 with an instrument module.

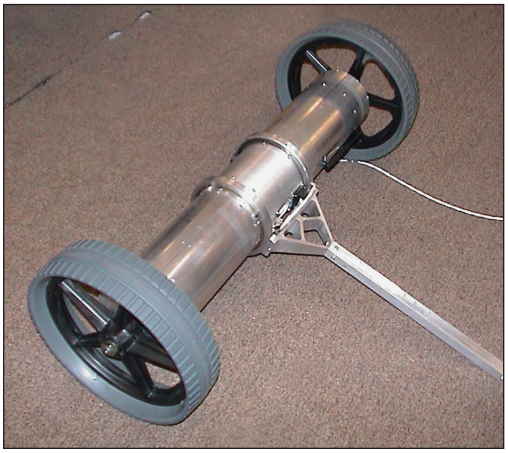

Figure 1. This **Two-Wheeled Vehicle** is a prototype of an Axel2.

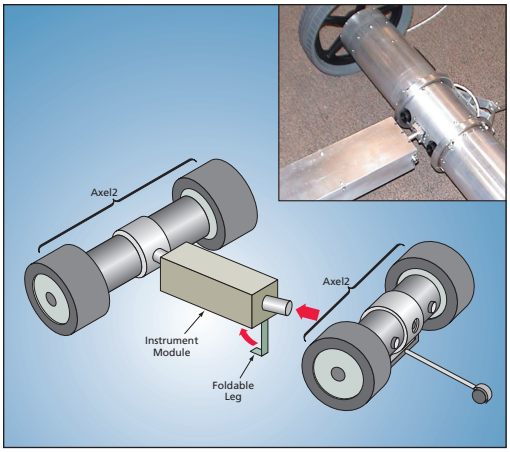

Figure 2. The **Prototype Axel2 and a Prototype Instrument Module** are depicted here during a docking maneuver that ends in coupling at the module interface.

Information on the Axel*n* software has become available since the prior article was published. To enable self-diagnosis and automatic reconfiguration of modular hardware, the architecture of the Axel*n* software provides for autonomous adaptation of the software to the hardware reconfiguration. More specifically, an Axel*n* uses software that can determine when physical reconfiguration is necessary (e.g., in response to task requirements or hardware failures), controls the hardware reconfiguration, and reconfigures itself to conform to the changed hardware configuration.

The capability for autonomous reconfiguration of the hardware depends heavily on the supporting software. One of the goals of the development of the Axel*n* system is to simplify and generalize through modularity. The reconfigurable software architecture mirrors the modularity of the hardware by providing that, as hardware modules are connected or disconnected, associated software modules are also put into or taken out of operation.

This work was done by Ayanna Howard, Issa Nesnas, Barry Werger, Daniel Helmick of Caltech; Murray Clark and Raymond Christian of Arkansas Tech; and Raymond Cipra of Purdue University for NASA's Jet Propulsion Laboratory. For more information, contact iaoffice@jpl.nasa.gov.

NPO-30890

Thermostatic Valves Containing Silicone-Oil Actuators

NASA's Jet Propulsion Laboratory, Pasadena, California

Flow-splitting and flow-mixing thermally actuated spool valves have been developed for controlling flows of a heat-transfer fluid in a temperature-regulation system aboard the Mars Science Laboratory (MSL) rover. Valves like these could also be useful in terrestrial temperature-regulation systems, including automobile air-conditioning systems and general refrigeration systems. These valves are required to provide smoother actuation over a wider temperature range than the flow-splitting, thermally actuated spool valves used in the Mars Explorer Rover (MER). Also, whereas the MER valves are unstable (tending to oscillate) in certain transition temperature ranges, these valves are required not to oscillate.

The MER valves are actuated by thermal expansion of a wax against spring-loaded piston rods (as in common automotive thermostats). The MSL valves contain similar actuators that utilize thermal expansion of a silicone oil, because silicone-oil actuators were found to afford greater and more nearly linear displacements, needed for smoother actuation, over the required wider temperature range. The MSL valves also feature improved spool designs that reflect greater understanding of fluid dynamics, consideration of pressure drops in valves, and a requirement for balancing of pressures in different flow branches.

This work was done by Pradeep Bhandari, Gajanana C. Birur, David P. Bame, Paul B. Karlmann, and Mauro Prina of Caltech and William Young and Richard Fisher of Pacific Design Technology for NASA's Jet Propulsion Laboratory.

In accordance with Public Law 96-517, the contractor has elected to retain title to this invention. Inquiries concerning rights for its commercial use should be addressed to:

Innovative Technology Assets Management
JPL
Mail Stop 202-233
4800 Oak Grove Drive
Pasadena, CA 91109-8099
E-mail: iaoffice@jpl.nasa.gov

Refer to NPO-45843, volume and number of this NASA Tech Briefs *issue, and the page number.*

Improving Heat Flux Performance of Flat Surface in Spray-Cooling Systems

Goddard Space Flight Center, Greenbelt, Maryland

A method has been developed for improving heat flux performance relative to flat surfaces in spray-cooling systems. Similar enhancement techniques have been used for convective heat transfer, but, to the best knowledge at the time of this reporting, never spray cooling of foam. Previous studies have shown that spray-cooling heat flux enhancements may be attained using enhanced surfaces. However, most enhanced surface spray-cooling studies have been limited to extended and/or embedded surface structures. This study investigates the effect of foam on spraycooling heat flux.

The foam used was graphite Poco Foam. The foam piece was attached to a copper block with a cross-sectional area of 2 cm^2 using high-thermal-conductivity epoxy as the thermal interface material. Measurements were also obtained on a heater block with a flat surface for purposes of baseline comparison. A 2×2 nozzle array was used with PF-5060 as the working fluid. Thermal performance data was obtained under nominally degassed conditions, with a chamber pressure of 41.4 kPa.

Results show that the highest heat flux attained was 113 W/cm^2 using the graphite Poco Foam. The use of the foam does not require a significant amount of time dedicated to machining the heat exchange surface, and thus is a time-efficient enhancement technique. In addition, with foam, the thermally controlled surface does not experience abrupt catastrophic failure.

This work was done by Eric A. Silk of Goddard Space Flight Center. For further information, contact the Goddard Innovative Partnerships Office at (301) 286-5810. GSC-15553-1

Treating Fibrous Insulation To Reduce Thermal Conductivity

Lyndon B. Johnson Space Center, Houston, Texas

A chemical treatment reduces the convective and radiative contributions to the effective thermal conductivity of porous fibrous thermal-insulation tile. The net effect of the treatment is to coat the surfaces of fibers with a mixture of transition-metal oxides (TMOs) without filling the pores. The TMO coats reduce the cross-sectional areas available for convection while absorbing and scattering thermal radiation in the pores, thereby rendering the tile largely opaque to thermal radiation.

The treatment involves a sol-gel process: A solution containing a mixture of transition-metal-oxide-precursor salts plus a gelling agent (e.g., tetraethylorthosilicate) is partially cured, then, before it visibly gels, is used to impregnate the tile. The solution in the tile is gelled, then dried, and then the tile is fired to convert the precursor salts to the desired mixed TMO phases. The amounts of the various TMOs ultimately incorporated into the tile can be tailored via the concentrations of salts in the solution, and the impregnation depth can be tailored via the viscosity of the solution and/or the volume of the solution relative to that of the tile. The amounts of the TMOs determine the absorption and scattering spectra.

This work was done by Alfred Zinn and Ryan Tarkanian of The Boeing Co. for Johnson Space Center. Further information is contained in a TSP (see page 1).

Title to this invention, covered by U.S. Patent No. 7,198,839 B2, has been waived under the provisions of the National Aeronautics and Space Act {42 U.S.C. 2457 (f)}. Inquiries concerning licenses for its commercial development should be addressed to:

The Boeing Company
5301 Bolsa Ave,
Huntington Beach, CA 92647-2099

Refer to MSC-23394-1, volume and number of this NASA Tech Briefs *issue, and the page number.*

Silica-Aerogel Composites Opacified With $La_{0.7}Sr_{0.3}MnO_3$

Sizes of $La_{0.7}Sr_{0.3}MnO_3$ particles affect their effectiveness as opacifiers.

Marshall Space Flight Center, Alabama

As part of an effort to develop improved lightweight thermal-insulation tiles to withstand temperatures up to 1,000 °C, silica aerogel/fused-quartz-fiber composite materials containing $La_{0.7}Sr_{0.3}MnO_3$ particles as opacifiers have been investigated as potentially offering thermal conductivities lower than those of the otherwise equivalent silica-aerogel composite materials not containing $La_{0.7}Sr_{0.3}MnO_3$ particles. The basic idea of incorporating opacifying particles into silica-aerogels composite to reduce infrared radiative contributions to thermal conductivities at high temperatures is not new: it has been reported in a number of previous *NASA Tech Briefs* articles. What is

new here is the selection of $La_{0.7}Sr_{0.3}MnO_3$ particles as candidate opacifiers that, in comparison with some prior opacifiers (carbon black and metal nanoparticles), are more thermally stable.

The preparation of a composite material of the present type includes synthesis of the silica-aerogel component in a sol-gel process. The $La_{0.7}Sr_{0.3}MnO_3$ particles, made previously in a separate process, are mixed into the sol, which is then cast onto fused-quartz-fiber batting. Then the aerogel-casting solution is poured into the mold, where it permeates the silica fiber felt. After the sol has gelled, the casting is aged and then subjected to supercritical drying to convert the gel to the final aerogel form.

The separate process for making the $La_{0.7}Sr_{0.3}MnO_3$ particles begins with the slow addition of corresponding proportions of $La(CH_3COOH)_3$, $Mn(CH_3COOH)_3$, and $Sr(NO_3)_2$ to a solution of H_2O_2 in H_2O. The solution is then peptized by drop-wise addition of NH_4OH to obtain a sol. Next, the sol is dried in an oven at a temperature of 120 °C to obtain a glassy solid. The solid is calcined at 700 °C to convert it to $La_{0.7}Sr_{0.3}MnO_3$. Then $La_{0.7}Sr_{0.3}MnO_3$ particles are made by ball-milling the calcined solid.

The effectiveness of $La_{0.7}Sr_{0.3}MnO_3$ particles as opacifiers and thermal-conductivity reducers depends on the statistical distribution of particle sizes as well as the relative proportions of $La_{0.7}Sr_{0.3}MnO_3$ and aerogel. For experiments performed thus far, samples of aerogel/fiber composites were formulated to have, variously, silica target density of 0.07 or 0.14 g/cm^3 and to contain 30 percent of $La_{0.7}Sr_{0.3}MnO_3$ in average particle size of 0.3 or 3 μm. The thermal conductivities of the samples containing the 3-μm $La_{0.7}Sr_{0.3}MnO_3$ particles were found to be lower than those of the samples containing the 0.3-μm $La_{0.7}Sr_{0.3}MnO_3$ particles. The optimum particle size is believed to be between 1 and 5 μm.

This work was done by Wendell Rhine, Andrew Polli, and Kiranmayi Deshpande of Aspen Aerogels, Inc. for Marshall Space Flight Center. For further information, contact Sammy Nabors, MSFC Commercialization Assistance Lead, at sammy.a.nabors@nasa.gov. Refer to MFS-32587-1.

Cyclic Oxidation Behavior of CuCrAl Cold-Sprayed Coatings for Reusable Launch Vehicles

John H. Glenn Research Center, Cleveland, Ohio

The next generation of reusable launch vehicles is likely to use GRCop-84 [Cu-8(at.%)Cr-4%Nb] copper alloy combustion liners. The application of protective coatings on GRCop-84 liners can minimize or eliminate many of the environmental problems experienced by uncoated liners and significantly extend their operational lives and lower operational cost. A newly developed Cu-23 (wt.%) Cr-5% Al (CuCrAl) coating, shown to resist hydrogen attack and oxidation in an as-cast form, is currently being considered as a protective coating for GRCop-84. The coating was deposited on GRCop-84 substrates by the cold spray deposition technique, where the CuCrAl was procured as gas-atomized powders. Cyclic oxidation tests were conducted between 773 and 1,073 K to characterize the coated substrates.

The coating proved to be effective in preventing the cyclic oxidation of the substrate for up to 1,000 cycles. The coated substrates showed no significant weight loss in comparison to uncoated specimens, which lost between 60 to 80 percent of its original weight with much lower lives. The coating was adherent to the substrate at all temperatures, whereas the uncoated GRCop-84 showed excessive spallation of the oxide scale. It is anticipated that the use of this alloy can extend the operational life of the liner, which translates to increased component reliability, shorter depot maintenance turnaround time, and lower operational cost. Additionally, engines using CuCrAl-coated GRCop-84 combustion liners could operate at higher temperatures, thereby resulting in its increased thermal efficiency.

This work was done by Sai Raj of Glenn Research Center and J. Karthikeyan of ASB Industries. Further information is contained in a TSP (see page 1).

Inquiries concerning rights for the commercial use of this invention should be addressed to NASA Glenn Research Center, Innovative Partnerships Office, Attn: Steve Fedor, Mail Stop 4–8, 21000 Brookpark Road, Cleveland, Ohio 44135. Refer to LEW-18330-1.

Ceramic Fiber Structures for Cryogenic Load-Bearing Applications

Woven or braided fibers resist embrittlement under cryogenic conditions, enabling ultralow-temperature applications.

John H. Glenn Research Center, Cleveland, Ohio

This invention is intended for use as a load-bearing device under cryogenic temperatures and/or abrasive conditions (i.e., during missions to the Moon). The innovation consists of small-diameter, ceramic fibers that are woven or braided into devices like ropes, belts, tracks, or cables. The fibers can be formed from a variety of ceramic materials like silicon carbide, carbon, aluminosilicate, or aluminum oxide. The fiber architecture of the weave or braid is determined by both the fiber properties and the mechanical requirements of the application. A variety of weave or braid

architectures is possible for this application. Thickness of load-bearing devices can be achieved by using either a 3D woven structure, or a layered, 2D structure. For the prototype device, a belt approximately 0.10 in. (0.25 cm) thick, and 3.0 in. (7.6 cm) wide was formed by layering and stitching a 2D aluminosilicate fiber weave. The circumferential length of the 2D, layered belt was approximately 36 in. (91 cm).

To demonstrate the resistance to abrasion while under load, the ceramic fiber belt was installed on two aluminum spools that were mounted in an Instron load frame. Both spools were completely enclosed in a Lexan box within the load frame. Bearings were used at each end of the spool shafts to allow the spools to spin freely while a load was applied. The lower spool, which was secured to the stationary head of the load frame, was also attached to a small motor to drive the rollers. The upper spool was attached to the movable crosshead of the Instron frame to apply a load to the belt while it was rolling. JSC1a, a highly abrasive lunar regolith simulant, was added to the Lexan box. Enough JSC1a was placed in the bottom of the box to allow the belt to contact and pick up the dust as it traveled around the lower spool. The track was exposed to the dust while rolling under load for several hours to simulate relevant rover mission duration. After 12.5 hours of exposure to the lunar simulant, under loads varying between 50 and 100 N, no elongation or mechanical creep of the belt was measured. Under these loads, which were estimated to be comparable to those required for tracks on the lunar rover, there was no deformation or loss of load carrying ability.

To demonstrate flexibility under cryogenic conditions, individual fibers and fiber tows were exposed to cryogenic temperatures by being submerged in liquid nitrogen for 4 minutes, and then were flexure tested. Immediately upon removal from the liquid nitrogen, the fibers and tows were wrapped around mandrels of progressively smaller diameters. Both the fibers and the tows were successfully wrapped around wire mandrels with a diameter of approximately 0.02 in. (0.5 mm) without any breakage. The continuous ceramic belt that is envisioned for the lunar rover would be a closed-edge, multilayer weave with through thickness holes woven in place. The holes in the weave would engage the sprockets on the drive mechanism of the track device.

This work was done by Martha H. Jaskowiak and Andrew J. Eckel of Glenn Research Center. Further information is contained in a TSP (see page 1).

Inquiries concerning rights for the commercial use of this invention should be addressed to NASA Glenn Research Center, Innovative Partnerships Office, Attn: Steve Fedor, Mail Stop 4–8, 21000 Brookpark Road, Cleveland, Ohio 44135. Refer to LEW- 18364-1.

Elastomer Reinforced With Carbon Nanotubes

Lyndon B. Johnson Space Center, Houston, Texas

Elastomers are reinforced with functionalized, single-walled carbon nanotubes (SWNTs) giving them high-breaking strain levels and low densities. Cross-linked elastomers are prepared using amine-terminated, poly(dimethylsiloxane) (PDMS), with an average molecular weight of 5,000 daltons, and a functionalized SWNT.

Cross-link densities, estimated on the basis of swelling data in toluene (a dispersing solvent) indicated that the polymer underwent cross-linking at the ends of the chains. This thermally initiated cross-linking was found to occur only in the presence of the aryl alcohol functionalized SWNTs. The cross-link could have been via a hydrogen-bonding mechanism between the amine and the free hydroxyl group, or via attack of the amine on the ester linage to form an amide.

Tensile properties examined at room temperature indicate a three-fold increase in the tensile modulus of the elastomer, with rupture and failure of the elastomer occurring at a strain of 6.5.

This work was done by James M. Tour and Jared L. Hudson of Rice University and Ramanan Krishnamoorti of University of Houston for Johnson Space Center. For further information, contact the JSC Innovation Partnerships Office at (281) 483-3809.

In accordance with Public Law 96-517, the contractor has elected to retain title to this invention. Inquiries concerning rights for its commercial use should be addressed to:

William M. Rice University
Office of Technology Transfer
6100 Main Street
Houston, TX 77005
Phone No.: (713) 348-6188

Refer to MSC-24071-1, volume and number of this NASA Tech Briefs *issue, and the page number.*

Biologically Inspired Purification and Dispersion of SWCNTs

Lyndon B. Johnson Space Center, Houston, Texas

A biologically inspired method has been developed for (1) separating single-wall carbon nanotubes (SWCNTs) from other materials (principally, amorphous carbon and metal catalysts) in raw production batches and (2) dispersing the SWCNTs as individual particles (in contradistinction to ropes and bundles) in suspension, as required for a number of applications. Prior methods of purification and dispersal of SWCNTs involve, variously, harsh physical processes (e.g., sonication) or harsh chemical processes (e.g., acid reflux). These processes do not completely remove the undesired materials and do not disperse bundles and ropes into individual suspended SWCNTs. Moreover, these processes cut long SWCNTs into shorter pieces, yielding typical nanotube lengths between 150 and 250 nm.

In contrast, the present method does not involve harsh physical or chemical processes. The method involves the use of biologically derived dispersal agents (BDDAs) in an aqueous solution that is mechanically homogenized (but not sonicated) and centrifuged. The dense solid material remaining after centrifu-

gation is resuspended by vortexing in distilled water, yielding an aqueous suspension of individual, separated SWCNTs having lengths from about 10 to about 15 μm.

This work was done by Daniel L. Feeback of Johnson Space Center, Mark S. F. Clarke of University Space Research Association, and Pavel Nikolaev of GB Tech Inc. Further information is contained in a TSP (see page 1).

In accordance with Public Law 96-517, the contractor has elected to retain title to this invention. Inquiries concerning rights for its commercial use should be addressed to:

USRA
10227 Wincopin Circle, Suite 212,
Columbia, MD 21044

Refer to MSC-23322-1, volume and number of this NASA Tech Briefs *issue, and the page number.*

A Technique for Adjusting Eigenfrequencies of WGM Resonators

NASA's Jet Propulsion Laboratory, Pasadena, California

A simple technique has been devised for making small, permanent changes in the eigenfrequencies (resonance frequencies) of whispering-gallery-mode (WGM) dielectric optical resonators that have high values of the resonance quality factor (Q). The essence of the technique is to coat the resonator with a thin layer of a transparent polymer having an index of refraction close to that of the resonator material.

Successive small frequency adjustments can be made by applying successive coats. The technique was demonstrated on a calcium fluoride resonator to which successive coats of a polymer were applied by use of a hand-made wooden brush. To prevent temperature-related frequency shifts that could interfere with the verification of the effectiveness of this technique, the temperature of the resonator was stabilized by means of a three-stage thermoelectric cooler. Measurements of the resonator spectrum showed the frequency shifts caused by the successive coating layers.

This work was done by Dmitry Strekalov, Anatoliy Savchenkov, Lute Maleki, Andrey Matsko, Vladimir Iltchenko, and Jan Martin of Caltech for NASA's Jet Propulsion Laboratory. Further information is contained in a TSP (see page 1).

In accordance with Public Law 96-517, the contractor has elected to retain title to this invention. Inquiries concerning rights for its commercial use should be addressed to:

Innovative Technology Assets Management
JPL
Mail Stop 202-233
4800 Oak Grove Drive
Pasadena, CA 91109-8099
(818) 354-2240
E-mail: iaoffice@jpl.nasa.gov

Refer to NPO-44383, volume and number of this NASA Tech Briefs *issue, and the page number.*

Low-Pressure, Field-Ionizing Mass Spectrometer

This lightweight, low-power instrument functions well in a low-grade (partial) vacuum.

NASA's Jet Propulsion Laboratory, Pasadena, California

A small mass spectrometer utilizing a miniature field ionization source is now undergoing development. It is designed for use in a variety of applications in which there are requirements for a lightweight, low-power-consumption instrument that can analyze the masses of a wide variety of molecules and ions. The device can operate without need for a high-vacuum, carrier-gas feed radioactive ionizing source, or thermal ionizer. This mass spectrometer can operate either in the natural vacuum of outer space or on Earth at any ambient pressure below 50 torr (below about 6.7 kPa) — a partial vacuum that can easily be reached by use of a small sampling pump. This mass spectrometer also has a large dynamic range — from singly charged small gas ions to deoxyribonucleic acid (DNA) fragments larger than 10^4 atomic mass units — with sensitivity adequate for detecting some molecules and ions at relative abundances of less than one part per billion.

This instrument (see figure) includes a field ionizer integrated with a rotating-field mass spectrometer (RFMS). The field ionizer effects ionization of a type characterized as "soft" in the art because it does not fragment molecules or initiate avalanche arcing. What makes the "soft" ionization mode possible is that the distance between the ionizing electrodes is less than mean free path for ions at the maximum anticipated operat-

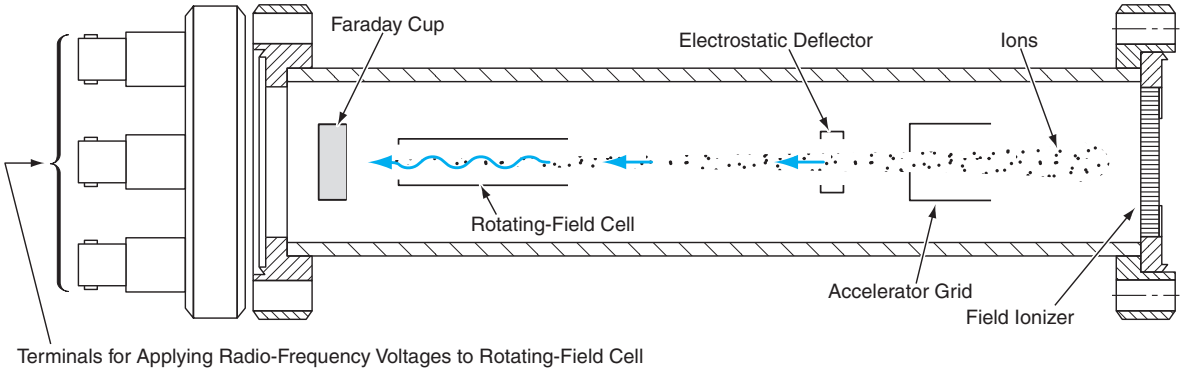

A **Field Ionizer and a Rotating-Field Mass Spectrometer** are integrated into a single instrument that has a mass <1 kg and a power consumption <5 W.

ing pressure, so that the ionizer always operates on the non-breakdown side of the applicable Paschen curve (a standard plot of breakdown potential on the ordinate and pressure electrode separation on the abscissa).

The field ionizer in this instrument is fabricated by micromachining a submicron-thick membrane out of an electrically nonconductive substrate, coating the membrane on both sides to form electrodes, then micromachining small holes through the electrodes and membrane. Because of the submicron electrode separation, even a potential of only 1 V applied between the electrodes gives rise to an electric field with a strength of in excess of a megavolt per meter — strong enough to ionize any gas molecules passing through the holes.

An accelerator grid and an electrostatic deflector focus the ions from the field ionizer into the rotating-field cell of the RFMS. The potentials applied to the electrodes of the cell to generate the rotating electric field typically range from 1 to 13 V. The ions travel in well-defined helices within this cell, after which they are collected in a Faraday cup. The mass of most of the molecules reaching the Faraday cup decreases with increasing frequency of rotation of the electric field in the cell. Therefore, the frequency of rotation of the electric field is made to vary in order to scan through a desired range of ion masses: For example, lightweight gas molecules are scanned at frequencies in the megahertz range, while DNA and other large organic molecules are scanned at kilohertz frequencies.

The current of accelerated ions is attenuated by collisions between these ions and the much slower (thermal) background gas molecules. In a typical case of operation at 5 Torr, an initial ion-beam current of about 10 nA would be attenuated to about 40 pA. However, the instrument could still afford adequate sensitivity because the electric current of ions collected by the Faraday cup is read by use of an electrometer that can resolve a current of the order of a femtoampere. In certain cases of low vacuum (10^{-5} Torr), a channel electron multiplier (CEM) plate could also be utilized in a single ion detection mode.

This work was done by Frank Hartley and Steven Smith of Caltech for NASA's Jet Propulsion Laboratory. Further information is contained in a TSP (see page 1).

In accordance with Public Law 96-517, the contractor has elected to retain title to this invention. Inquiries concerning rights for its commercial use should be addressed to:

Innovative Technology Assets Management
JPL
Mail Stop 202-233
4800 Oak Grove Drive
Pasadena, CA 91109-8099
(818) 354-2240
E-mail: iaoffice@jpl.nasa.gov

Refer to NPO-30245, volume and number of this NASA Tech Briefs *issue, and the page number.*

Modifying Operating Cycles To Increase Stability in a LITS

Microwave-interrogation time can be increased while maintaining optimum lamp duty cycle.

NASA's Jet Propulsion Laboratory, Pasadena, California

The short-term instability in the frequency of a linear-ion-trap frequency standard (LITS) can be reduced by modifying two cycles involved in its operation: (1) the bimodal (bright/dim) cycle of a plasma discharge lamp used for state preparation and detection and (2) a microwave-interrogation cycle. The purpose and effect of the modifications is to enable an increase in the microwave-interrogation cycle time, motivated by the general principle that the short-term uncertainty or instability decreases with increasing microwave-interrogation time. Stated from a slightly different perspective, the effect of modifications is to enable the averaged LITS readings to settle to their long-term stability over a shorter total observation time.

The basic principles of a LITS were discussed in several *NASA Tech Briefs* articles. Here are recapitulated only those items of background information necessary to place the present modifications in context. A LITS includes a microwave local oscillator, the frequency of which is stabilized by comparison with the frequency of a ground-state hyperfine transition of $^{199}Hg^{+}$ ions. In a LITS of the type to which the modifications apply, the comparison involves a combination of optical and microwave excitation and interrogation of the ions in two collinear ion traps: a quadrupole trap wherein the optical excitation used for state preparation and detection takes place, and a multipole (e.g., 12-pole) trap wherein the microwave interrogation of the "clock" transition takes place. The ions are initially loaded into the quadrupole trap and are thereafter shuttled between the two traps. This concludes the background information.

One source of systematic frequency error is an AC Stark shift caused by light present during microwave interrogation. To minimize this source of error, most stray light is suppressed by design, and heretofore, the microwave-interrogation time has been limited to the dim portion of the bimodal lamp cycle. It has now been learned that it is not necessary to limit the microwave interrogation to the dim portion of the lamp cycle because the separation of the two collinear ion traps is such that very little light from the lamp reaches the multipole trap wherein the microwave interrogation takes place. Indeed, the lamp-light-attenuation factor associated with the separation of the collinear ion traps is greater than the ratio between the bright and dim lamp intensities. The abandonment of this limitation creates an option to operate the lamp at an optimum duty cycle and to perform the microwave interrogation for a longer time, as described next.

The equilibrium temperature of the lamp depends on the ambient temperature and the lamp duty cycle. For each lamp, it is possible to empirically determine an equilibrium temperature (and, hence, a duty cycle) that is optimum in the sense that it maximizes the signal-to-noise ratio (SNR) during microwave interrogation. Hence, one of the modifications is to set the bimodal lamp operating cycle to the optimum duty cycle. The other modification is to increase the microwave-interrogation time to a desired integer multiple of the lamp cycle time. (The multiple must have an integer value because it is still necessary to synchronize the optical and microwave operating cycles.) The size of the integer multiple is subject to an over-

all limit determined by the quantum-coherence time of the $^{199}Hg^{+}$ ions and the characteristic stability time of the microwave source.

The following results have been reported from experiments performed on a LITS to demonstrate these modifications: The best short-term fractional frequency instability achieved with a typical microwave-interrogation time of 6 s in the unmodified bimodal lamp cycle was between 7 and $10 \times 10^{-14}\tau^{-1/2}$, where τ is the averaging (observation) time in seconds. The use of the modified lamp mode and a microwave-interrogation time of 30 s resulted in a short-term fractional instability of 5 and $10 \times 10^{-14}\tau^{-1/2}$. To put these numbers in perspective, it was calculated that the time for the LITS to settle to a fractional frequency instability of 10^{-16} would be about 8.4 days without the modifications or 2.9 days with the modifications.

This work was done by Eric Burt and Robert Tjoelker of Caltech for NASA's Jet Propulsion Laboratory. For more information, contact iaoffice@jpl.nasa.gov. NPO-44271

Chamber for Simulating Martian and Terrestrial Environments

Temperature, pressure, and simulated solar radiation can be controlled over wide ranges.

John F. Kennedy Space Center, Florida

An apparatus for simulating the environment at the surface of Mars has been developed. Within the apparatus, the pressure, gas composition, and temperature of the atmosphere; the incident solar visible and ultraviolet (UV) light; and the attenuation of the light by dust in the atmosphere can be simulated accurately for any latitude, season, or obliquity cycle over the entire geological history of Mars. The apparatus also incorporates instrumentation for monitoring chemical reactions in the simulated atmosphere. The apparatus can be used for experiments in astrobiology, geochemistry, aerobiology, and aerochemistry related to envisioned robotic and human exploration of Mars. Moreover, the apparatus can be easily adapted to enable similar experimentation under environmental conditions of (1) the surfaces of moons, asteroids, and comets, and (2) the upper atmospheres of planets other than Mars: in particular, it can be made to simulate conditions anywhere in the terrestrial atmosphere at altitudes up to about 100 km.

The apparatus (see figure) includes a cylindrical stainless-steel chamber, wherein the simulated atmospheric pressure is maintained between set points by means of a vacuum pump and a throttle valve controlled by an electronic pressure controller. The pressure can be set at any level from ambient down to 0.1 mb (100 Pa). A commercially available Martian-atmosphere-simulating mixture of gases (95.54% CO_2 + 2.7% N_2 + 1.6% Ar + 0.13% O_2 + 0.03% H_2O) is delivered from a tank to the chamber through a mass-flow controller. The primary temperature-control system is a commercially available unit that includes a cold plate in the chamber and that utilizes liquid nitrogen to reach the

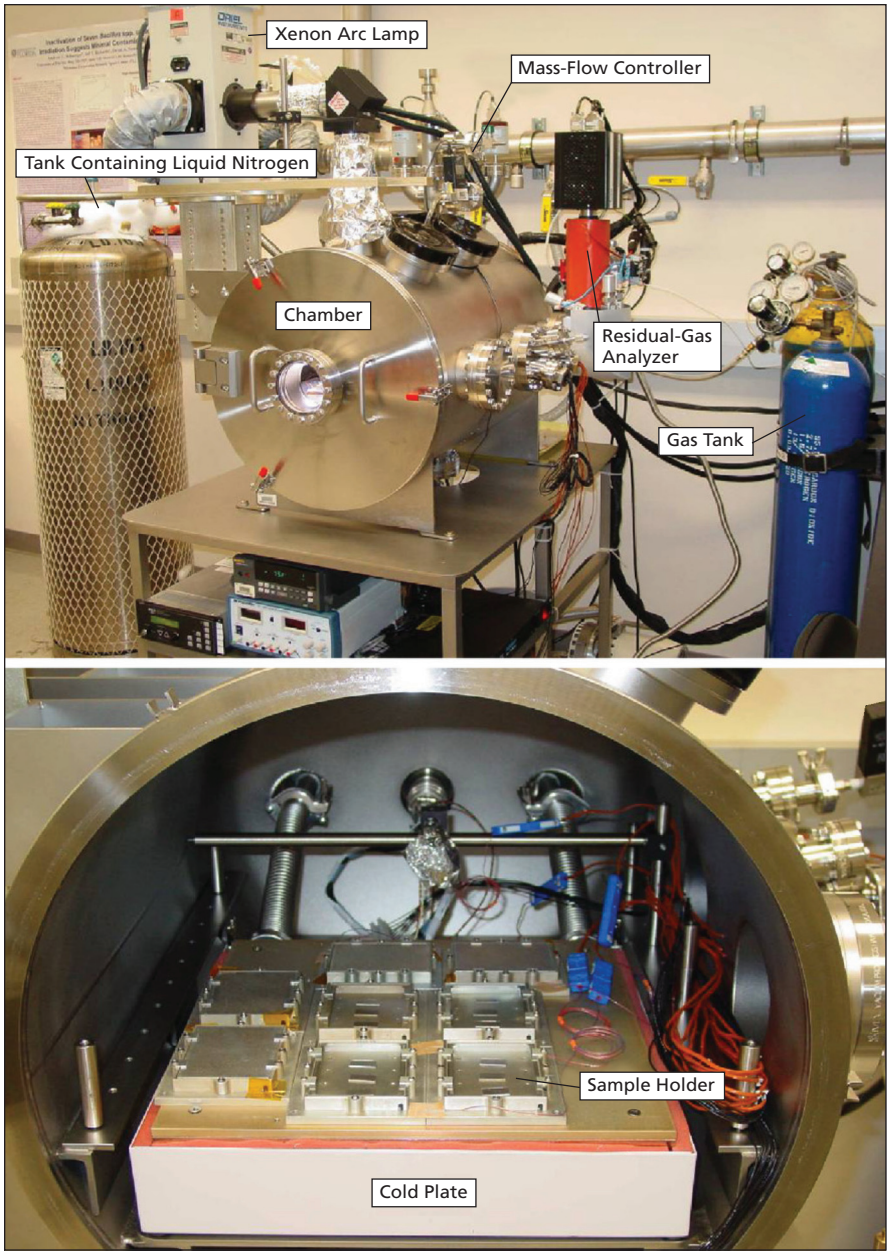

This **Laboratory Apparatus** reproduces, inside the chamber, environmental conditions like those on the Martian surface or in the upper terrestrial atmosphere.

lowest temperatures. The temperature-control system can be programmed to maintain any temperature between –100 and +160 °C and/or to impose diurnal heating and cooling cycles.

Ultraviolet (UV), visible (VIS), and near-infrared light (IR) are supplied to the inside of the chamber through fused-silica glass ports. In the original Mars version of the apparatus, the UV light is generated by a xenon-arc lamp and can be adjusted to any realistic current or ancient Martian UV flux density. To suppress spurious thermal IR radiation, a water filter between the xenon-arc lamp and the chamber attenuates near- and mid-infrared light. The light-attenuating effects of dust in the atmosphere are simulated by means of a series of neutral-density filters, ranging from an optical depth of 0.1 (representing a dust-free sky) to an optical depth of 3.5 (representing a global dust storm).

This work was done by Andrew C. Schuerger of the University of Florida for Kennedy Space Center. Further information is contained in a TSP (see page 1). ***KSC-13190***

Algorithm for Detecting a Bright Spot in an Image

Corrections for background intensity and dark current are included.

NASA's Jet Propulsion Laboratory, Pasadena, California

An algorithm processes the pixel intensities of a digitized image to detect and locate a circular bright spot, the approximate size of which is known in advance. The algorithm is used to find images of the Sun in cameras aboard the Mars Exploration Rovers. (The images are used in estimating orientations of the Rovers relative to the direction to the Sun.) The algorithm can also be adapted to tracking of circular shaped bright targets in other diverse applications.

The first step in the algorithm is to calculate a dark-current ramp — a correction necessitated by the scheme that governs the readout of pixel charges in the charge-coupled-device camera in the original Mars Exploration Rover application. In this scheme, the fraction of each frame period during which dark current is accumulated in a given pixel (and, hence, the dark-current contribution to the pixel image-intensity reading) is proportional to the pixel row number. For the purpose of the algorithm, the dark-current contribution to the intensity reading from each pixel is assumed to equal the average of intensity readings from all pixels in the same row, and the factor of proportionality is estimated on the basis of this assumption. Then the product of the row number and the factor of proportionality is subtracted from the reading from each pixel to obtain a dark-current-corrected intensity reading.

The next step in the algorithm is to determine the best location, within the overall image, for a window of $N \times N$ pixels (where N is an odd number) large enough to contain the bright spot of interest plus a small margin. (In the original application, the overall image contains 1,024 by 1,024 pixels, the image of the Sun is about 22 pixels in diameter, and N is chosen to be 29.)

The window is placed at a given position within the overall image. A weighted average of the intensities of the $4N - 4$ outer pixels of the window is taken as an estimate of background intensity and subtracted from a weighted average of the intensities of the remaining inner $(N-2) \times (N-2)$ pixels of the window to obtain a background-corrected weighted sum of pixel intensities for the window. The weighted averages are simply pixel-intensity averages multiplied by common denominators so as to obviate floating-point arithmetic operations and thereby accelerate computations. The window is then moved to an adjacent column position, and weighted averages for the new position are calculated from the previous weighted averages by adding the appropriate values for the new outer and inner pixels and subtracting the corresponding values for the pixels that have been left behind or changed in status between the inner and the outer. This process is repeated until the computations have been performed for all possible window positions. The position that yields the highest background-corrected weighted sum of pixel intensities is assumed to contain the bright spot of interest (the image of the Sun in the original application), and the window is then used to locate the bright spot more precisely as described next.

Within the inner $(N-2) \times (N-2)$ portion of the window, the position of the bright spot is determined by means of a simple centroid calculation, using the background-corrected pixel intensities. Because the window position selected as described above may not necessarily be the optimum one, the centroid calculation is performed twice in an iterative process: For the second centroid calculation, the window is re-centered on the centroid determined by the first centroid calculation.

This work was done by Carl Christian Liebe of Caltech for NASA's Jet Propulsion Laboratory.

The software used in this innovation is available for commercial licensing. Please contact Karina Edmonds of the California Institute of Technology at (626) 395-2322. Refer to NPO-41801.

Extreme Programming: Maestro Style

Modifications have been made to suit a specific development environment.

NASA's Jet Propulsion Laboratory, Pasadena, California

"Extreme Programming: Maestro Style" is the name of a computer-programming methodology that has evolved as a custom version of a methodology, called "extreme programming" that has been practiced in the software industry since the late 1990s. The name of this version reflects its origin in the work of the Maestro team at NASA's Jet Propulsion Laboratory that develops software for Mars exploration missions.

Extreme programming is oriented toward agile development of software resting on values of simplicity, communication, testing, and aggressiveness. Extreme programming involves use of methods of rapidly building and disseminating institutional knowledge among members of a computer-programming team to give all the members a shared view that matches the view of the customers for whom the software system is to be developed. Extreme programming includes frequent planning by programmers in collaboration with customers, continually examining and rewriting code in striving for the simplest workable software designs, a system metaphor (basically, an abstraction of the system that provides easy-to-remem-

ber software-naming conventions and insight into the architecture of the system), programmers working in pairs, adherence to a set of coding standards, collaboration of customers and programmers, frequent verbal communication, frequent releases of software in small increments of development, repeated testing of the developmental software by both programmers and customers, and continuous interaction between the team and the customers.

The environment in which the Maestro team works requires the team to quickly adapt to changing needs of its customers. In addition, the team cannot afford to accept unnecessary development risk. Extreme programming enables the Maestro team to remain agile and provide high-quality software and service to its customers. However, several factors in the Maestro environment have made it necessary to modify some of the conventional extreme-programming practices. The single most influential of these factors is that continuous interaction between customers and programmers is not feasible. The major resulting differences between the Maestro and conventional versions of extreme programming are the following:

- Because customers are not always available for planning sessions, members of the team act on behalf of customers during these sessions.
- In an elaboration of the frequent-planning and incremental-release concept, releases and planning meetings are synchronized with a fixed one-week iteration cycle that facilitates maintenance of focus on the development task.
- Metaphors are occasionally used as needed in specific instances, but the conventional extreme-programming concept of a system metaphor is abandoned as not being helpful.
- In a departure from the simplest-design rule, the team sometimes develops software infrastructure that affords capabilities, beyond those required in the current iteration, that may be useful later in the development process.
- In the absence of continuous involvement of customers and of frequent testing of software by customers, there is heavy reliance on automated testing.

This work was done by Jeffrey Norris, Jason Fox, Kenneth Rabe, I-Hsiang Shu, and Mark Powell of Caltech for NASA's Jet Propulsion Laboratory. Further information is contained in a TSP (see page 1).

The software used in this innovation is available for commercial licensing. Please contact Karina Edmonds of the California Institute of Technology at (626) 395-2322. Refer to NPO-41811.

Adaptive Behavior for Mobile Robots

A robotic system attempts to both preserve itself and progress toward a goal.

NASA's Jet Propulsion Laboratory, Pasadena, California

The term "System for Mobility and Access to Rough Terrain" (SMART) denotes a theoretical framework, a control architecture, and an algorithm that implements the framework and architecture, for enabling a land-mobile robot to adapt to changing conditions. SMART is intended to enable the robot to recognize adverse terrain conditions beyond its optimal operational envelope, and, in response, to intelligently reconfigure itself (e.g., adjust suspension heights or baseline distances between suspension points) or adapt its driving techniques (e.g., engage in a crabbing motion as a switchback technique for ascending steep terrain). Conceived for original application aboard Mars rovers and similar autonomous or semi-autonomous mobile robots used in exploration of remote planets, SMART could also be applied to autonomous terrestrial vehicles to be used for search, rescue, and/or exploration on rough terrain.

In SMART, controlling the motion of the robot, managing the "health" of the robot, and managing resources are considered as parts of a free-flow behavior hierarchy that autonomously adapts to changing conditions. Tasks that must be performed in the continuing development of SMART are to provide for safe, adaptive mobility on highly sloped terrain include:

- Determination of strategies for adaptive reconfiguration and driving that are nearly optimal with respect to safety and are computationally feasible for on-board implementation,
- Determination of a representation for uncertainty in sensing and prediction of the state of the robot and its environment, and
- Determination of resource-management strategies that mitigate such risks as those of the loss of battery power and/or drive motors.

SMART is based largely on a prior architecture denoted Biologically Inspired System for Map-based Autonomous Rover Control (BISMARC), which, in turn is based on a modified free-flow hierarchy. BISMARC has been used with success in a number of different simulated mission scenarios, wherein it has been demonstrated to afford capabilities for retrieving objects cached at multiple locations, fault tolerance on missions of long duration, and preparing terrain sites for habitation by humans. BISMARC includes provisions for all aspects of safety, self-maintenance, and achievement of goals, as needed to support a sustained presence on the surface of a remote planet.

BISMARC is organized as a two-level system. From stereoscopic images acquired by cameras aboard the robot, the first level generates hypotheses of motor actions. The second level processes these hypotheses, coupled with external and internal inputs, to generate control signals to drive the actuators on the robot.

The figure illustrates the free-flow action-selection hierarchy of BISMARC and SMART. The rectangular boxes represent behaviors, while the ovals represent sensory inputs (either fixed, direct, or derived). At the top are the high-level behaviors, including Don't Tip Over, Go to Goal, Avoid Obstacles, Preserve Motors, Warm Up, Get Power, and Sleep at Night. The intermediate-level behaviors (Change Center of Gravity, Avoid Obstacles, Rest, and Sleep) are designed to interact with both the short-term memory (which corresponds to perceived sensory stimuli), and the long-term memory (which encodes remembered sensory information). Control loops are prevented by use of temporal penalties, which constrain the system to repeat a given behavior no more than a predetermined number of times. The bottom-level behaviors (Tilt Arm, Change Shoulder Angles, Move, Rest, Stop, Sleep) fuse the sensory inputs and the activations of the higher-level behaviors in order to select appropriate actions for safety and achieving goals.

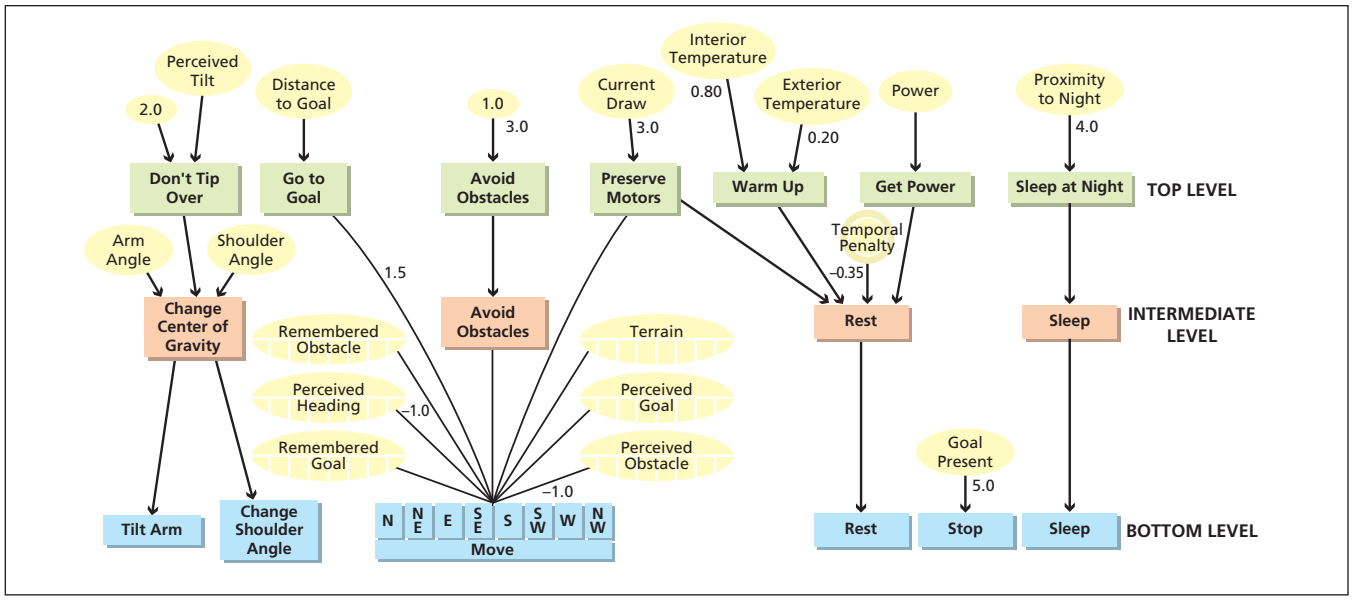

The **Free-Flow Action-Selection Hierarchy** includes multiple behaviors at different levels. The numerical values shown at several places are examples of weights assigned to inputs of behavioral modes. In general, such weights are changed as needed to adapt to changing or previously unknown environmental conditions.

Inputs to the behavioral nodes are calculated as weighted sums. In BISMARC, the weights are fixed; consequently, BISMARC is not capable of adaptation to changing conditions or to environments outside an original world model. In contrast, SMART includes a learning mechanism that adapts the weights to changing and previously unanticipated conditions: An algorithm, known in the art as the maximize collective happiness (MCH) algorithm, adjusts the weights in such a manner as to maintain the health of the robot while ensuring progress toward the goal.

This work was done by Terrance Huntsberger of Caltech for NASA's Jet Propulsion Laboratory.

The software used in this innovation is available for commercial licensing. Please contact Karina Edmonds of the California Institute of Technology at (626) 395-2322. Refer to NPO-40899.

Protocol for Communication Networking for Formation Flying

This protocol provides for adaptation to changing formation geometry and communication requirements.

NASA's Jet Propulsion Laboratory, Pasadena, California

An application-layer protocol and a network architecture have been proposed for data communications among multiple autonomous spacecraft that are required to fly in a precise formation in order to perform scientific observations. The protocol could also be applied to other autonomous vehicles operating in formation, including robotic aircraft, robotic land vehicles, and robotic underwater vehicles.

A group of spacecraft or other vehicles to which the protocol applies could be characterized as a precision-formation-flying (PFF) network, and each vehicle could be characterized as a node in the PFF network. In order to support precise formation flying, it would be necessary to establish a corresponding communication network, through which the vehicles could exchange position and orientation data and formation-control commands. The communication network must enable communication during early phases of a mission, when little positional knowledge is available. Particularly during early mission phases, the distances among vehicles may be so large that communication could be achieved only by relaying across multiple links. The large distances and need for omnidirectional coverage would limit communication links to operation at low bandwidth during these mission phases. Once the vehicles were in formation and distances were shorter, the communication network would be required to provide high-bandwidth, low-jitter service to support tight formation-control loops.

The proposed protocol and architecture, intended to satisfy the aforementioned and other requirements, are based on a standard layered-reference-model concept. The proposed application protocol would be used in conjunction with conventional network, data-link, and physical-layer protocols. The proposed protocol includes the ubiquitous Institute of Electrical and Electronics Engineers (IEEE) 802.11 medium access control (MAC) protocol to be used in the data-link layer. In addition to its widespread and proven use in diverse local-area networks, this protocol offers both (1) a random-access mode needed for the early PFF deployment phase and (2) a time-bounded-services mode needed during PFF-maintenance operations. Switching between these two modes could be controlled by upper-layer entities using standard link-management mechanisms.

Because the early deployment phase of a PFF mission can be expected to involve multihop relaying to achieve network connectivity (see figure), the proposed protocol includes the open shortest path

first (OSPF) network protocol that is commonly used in the Internet. Each spacecraft in a PFF network would be in one of seven distinct states as the mission evolved from initial deployment, through coarse formation, and into precise formation. Reconfiguration of the formation to perform different scientific observations would also cause state changes among the network nodes. The application protocol provides for recognition and tracking of the seven states for each node and for protocol changes under specified conditions to adapt the network and satisfy communication requirements associated with the current PFF mission phase. Except during early deployment, when peer-to-peer random-access discovery methods would be used, the application protocol provides for operation in a centralized manner.

The central communication node, denoted the "leader" spacecraft, would be selected so that its position in the formation tended to be spatially in the center. For example, PFF interferometry missions are typically configured with a single "combiner" that is centrally located relative to the other spacecraft. Selection of the spatially central node as the central communication node would leverage the special characteristics of the PFF networking problem domain in order to achieve high communication efficiency. In particular, when the spacecraft had positioned themselves into coarse formation, the IEEE 802.11 MAC protocol could be adapted from "distributed coordination function" (DCF) mode (a peer-to-peer random-access mode) to "point coordination function" (PCF) mode, in which the leader would act as the "point coordinator", so that time-bounded services needed to support time-critical control could be activated.

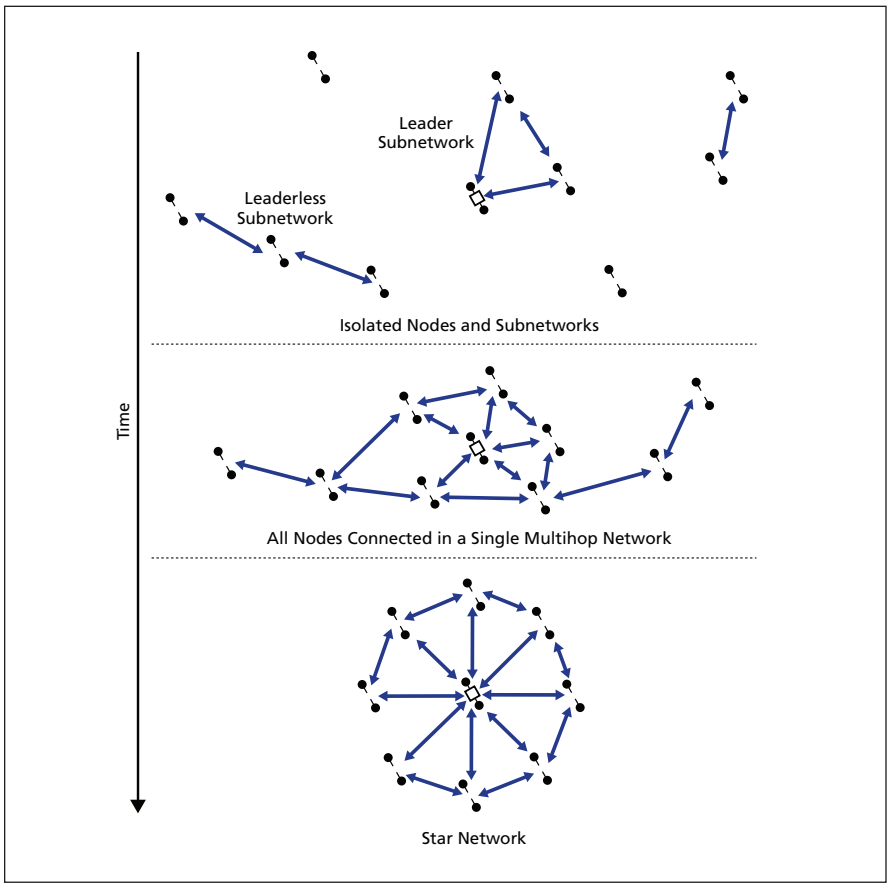

A **Communication Network** would evolve as spatially dispersed nodes moved into a coarse formation and then into a tightly controlled precise formation. The proposed protocol would enable communication among the nodes at all phases of evolution of the network.

Furthermore, if antenna patterns were biased to afford higher gain when the spacecraft were in coarse formation, the protocol could recognize these conditions and cause higher data rates to be used in communications. It should be noted that in conventional applications of the IEEE 802.11 MAC protocol in "ad hoc" networks, such *a priori* knowledge of antenna gain patterns and other features of network spatial configurations cannot be assumed and utilized. The predictability of the spacecraft formation would make it possible to utilize them in the proposed protocol.

This work was done by Esther Jennings, Clayton Okino, Jay Gao, and Loren Clare of Caltech for NASA's Jet Propulsion Laboratory. For more information, contact iaoffice@jpl.nasa.gov.
NPO-41486

Planning Complex Sequences Using Compressed Representations

Computation time and memory needed to generate schedules are greatly reduced.

NASA's Jet Propulsion Laboratory, Pasadena, California

A method that notably includes the use of compressed representations interleaved with non-compressed (time-line) representations of a general scheduling problem has been conceived as a means of increasing, by orders of magnitude, the speeds of computations needed for scheduling complex sequences of activities that include cycles wherein subsets of the activities and/or sequences are repeated. The method was originally intended to be used in scheduling large campaigns of scientific observations by instruments aboard a spacecraft. A typical such campaign could include observations of millions of targets, many observations to be made during long repeated passes. The method would also be useful on Earth for scheduling complex sequences of activities that include cycles.

The method is best summarized in the context of the original intended application, wherein the scheduling problem is formulated as that of selecting, from a candidate set of observations, those observations that cover as many target points as possible without oversubscrib-

ing energy and memory budgets. Inasmuch as observation opportunities repeat, the theoretical framework for evaluation of candidate solutions includes a cycle bound.

The method includes the use of an iterative optimization algorithm known in the art the "squeaky wheel optimization." This algorithm consists of the following steps:

1. Sort all of the target points according to priority.
2. Schedule each target point, greedily, in order of priority.
3. Increase priorities for those points that were omitted from the schedule in step 2.
4. Iterate by repeating from step 1.

Thus, points that are not initially scheduled have a greater probability of being scheduled on subsequent iterations because each time a point is not scheduled, its priority is increased, until eventually it becomes the first point scheduled.

At each iteration, points are considered in order of priority and observations considered in descending order of the contribution of each to coverage until a minimum acceptable level of coverage of each affected point has been scheduled. Only observations that cannot oversubscribe memory or energy and that respect transition duration constraints are considered. The asymptotic time complexity (in effect, the time needed to perform the computations) is of the order of a number proportional to $n\log(n)$ per iteration, where n is the number of points. This computation time is basically proportional to the time needed to sort the points according to priority.

For reasoning about multiple cycles, multiple cycles are used in representing energy and memory, but a single cycle is used in representing observations. The single-cycle representation can be characterized as compressed in that, relative to a time-line representation, it requires less memory to represent all possible observations over all cycles. Instead of listing all observations individually, one lists a single cycle of observations with labels that represent which observations belong to which cycles. The amount of memory needed to encode observations in this approach is proportional to the total number of observations.

This work was done by Steve Chien and Russell Knight of Caltech for NASA's Jet Propulsion Laboratory.

The software used in this innovation is available for commercial licensing. Please contact Karina Edmonds of the California Institute of Technology at (626) 395-2322. Refer to NPO-43768.

Self-Supervised Learning of Terrain Traversability From Proprioceptive Sensors

This system enables a vehicle to scan its surroundings and adapt to conditions by learning about them on the fly.

NASA's Jet Propulsion Laboratory, Pasadena, California

Robust and reliable autonomous navigation in unstructured, off-road terrain is a critical element in making unmanned ground vehicles a reality. Existing approaches tend to rely on evaluating the traversability of terrain based on fixed parameters obtained via testing in specific environments. This results in a system that handles the terrain well that it trained in, but is unable to process terrain outside its test parameters.

An adaptive system does not take the place of training, but supplements it. Whereas training imprints certain environments, an adaptive system would imprint terrain elements and the interactions amongst them, and allow the vehicle to build a map of local elements using proprioceptive sensors. Such sensors can include velocity, wheel slippage, bumper hits, and accelerometers. Data obtained by the sensors can be compared to observations from ranging sensors such as cameras and LADAR (laser detection and ranging) in order to adapt to any kind of terrain. In this way, it could sample its surroundings not only to create a map of clear space, but also of what kind of space it is and its composition.

By having a set of building blocks consisting of terrain features, a vehicle can adapt to terrain that it has never seen before, and thus be robust to a changing environment. New observations could be added to its library, enabling it to infer terrain types that it wasn't trained on. This would be very useful in alien environments, where many of the physical features are known, but some are not. For example, a seemingly flat, hard plain could actually be soft sand, and the vehicle would sense the sand and avoid it automatically.

This work was done by Max Bajracharya, Andrew B. Howard, and Larry H. Matthies of Caltech for NASA's Jet Propulsion Laboratory. For more information, contact iaoffice@jpl.nasa.gov. NPO-46601


NASA
National Aeronautics and
Space Administration